

Identifiable Energy-based Representations: An Application to Estimating Heterogeneous Causal Effects

Yao Zhang^{*†1}, Jeroen Berrevoets^{*1}, and Mihaela van der Schaar^{1,2,3}

¹University of Cambridge

²University of California, Los Angeles (UCLA)

³The Alan Turing Institute

August 9, 2021

Abstract

Conditional average treatment effects (CATEs) allow us to understand the effect heterogeneity across a large population of individuals. However, typical CATE learners assume all confounding variables are measured in order for the CATE to be identifiable. Often, this requirement is satisfied by simply collecting many variables, at the expense of increased sample complexity for estimating CATEs. To combat this, we propose an energy-based model (EBM) that learns a low-dimensional representation of the variables by employing a noise contrastive loss function. With our EBM we introduce a preprocessing step that alleviates the dimensionality curse for *any existing* model and learner developed for estimating CATE. We prove that our EBM keeps the representations partially identifiable up to some universal constant, as well as having universal approximation capability to avoid excessive information loss from model misspecification; these properties combined with our loss function, enable the representations to converge and keep the CATE estimation consistent. Experiments demonstrate the convergence of the representations, as well as show that estimating CATEs on our representations performs better than on the variables or the representations obtained via various benchmark dimensionality reduction methods.

1 Introduction

Average treatment effect (ATE) is arguably the most popular estimand in the causal inference literature. With the ATE, one measures if a treatment is effective on average over a population of individuals. However, even if we estimate an ATE accurately, we can not conclude if a treatment is beneficial for a particular individual. In order to get treatment effect estimates for one individual, we condition the ATE on the individual of interest, and arrive at the *conditional* average treatment effect (CATE). CATEs know successful applications in areas such as healthcare, education and economics.

While clinical trials represent the gold standard for causal inference, they often have a small number of individuals and narrow inclusion criteria, rendering them unsuitable for use in estimating the

^{*}Equal contribution.

[†]yz555@cam.ac.uk

causal effects conditional on some particular values of the confounding variables (covariates). On the other hand, observational datasets are becoming increasingly available, but require careful attention as they may have unobserved biases. There is growing interest in leveraging observational data to estimate CATEs, e.g., electronic healthcare records used to determine which patients should get what treatments, or school records to optimize educational policy in low- and high-income communities.

A fundamental assumption of no unobserved biases for causal inference on observational data is called the strong ignorability assumption [Rosenbaum and Rubin, 1983, 1984, 1985], also known as the unconfoundedness assumption. Ignorability assumes independence between the potential outcomes of interest and the treatment variable, conditional on the confounding covariates. Because this assumption is untestable, we often feed all the observed covariates into a regression model to estimate causal effects from observational data. To handle all these complex covariates in estimation, a variety of machine learning (ML) models [Alaa and van der Schaar, 2017; Shalit et al., 2017; Wager and Athey, 2018; Yoon et al., 2018; Hahn et al., 2020] and debiased ML methods (also known as CATE learners) [Nie and Wager, 2021; Chernozhukov et al., 2018; Foster and Syrgkanis, 2019; Künzel et al., 2019; Kennedy, 2020] have been proposed in recent literature.

Despite these advances, estimating CATEs remains challenging for a number of reasons, especially in the space of moderate or high dimensional covariates. First, we never observe two individuals with the same covariates. Moreover, the treated and control population are imbalanced due to treatment assignment bias. Furthermore, it is possible to observe no or very few treated or control individuals in some region of the data-space. When a CATE estimator’s expected risk is upper bounded by $Cn^{-\frac{1}{2}}$ for some positive constant C , we call it \sqrt{n} -consistent. Constructing such a \sqrt{n} -consistent CATE estimator is plausible if the CATE function is smooth or low-dimensional. However, the classic theory of nonparametric regression [Stone, 1980] implies that the smoothness requirement becomes more restrictive as the input dimension increases; see Section 2 for more detailed discussion.

1.1 Contributions

In this paper, we explore the assumption that the intrinsic dimension of the CATE function is lower than the observed covariates. We propose a representation learning method based on a partially randomized energy-based model (EBM) to embed the covariates into a low-dimensional space before estimating the CATE function. This preprocessing step can be used with any existing ML model and learner to reduce their dimensionality curse in CATE estimation. Theoretically, we show that the representation in the partially randomized EBM is *partially identifiable up to some universal constant* for any value of the covariates. Further, the EBM still has *universal approximation capability* for estimating any continuous covariates distribution, which avoids the problem of excessive information loss in parametric models due to model misspecification. To our best knowledge, identifying representations in deep learning models exactly is still infeasible. The existing theory settles on achieving weaker versions of identifiability with the help of some auxiliary information, e.g., time steps and class labels. Auxiliary information does not exist in most observational studies. We optimize the partially randomized EBM using a consistent noise contrastive loss function with sample splitting, which enables the representations to converge and keep the CATE estimation consistent.

Experiments on multiple datasets complement our theoretical results. We empirically validate the convergence of the representations with increasing sample size. We show estimating CATE based on our representations can achieve better performance than directly on the covariates or the representations obtained via various benchmark dimensionality reduction methods.¹

¹The code of our method is provided at: <https://github.com/jeroenbe/ebm-for-cate>.

2 Setup

Following [Neyman \[1923\]](#) and [Rubin \[1974\]](#), we use the potential outcomes framework to define causal effects. Consider an observational dataset $\mathcal{D} = \{O_i = (X_i, A_i, Y_i) : i \in [n]\}$, where $[n] = \{1, \dots, n\}$. Each individual i is described by a set of covariates $X_i \in \mathcal{X} \subseteq \mathbb{R}^d$, a binary treatment variable $A_i \in \mathcal{A} = \{0, 1\}$ and an observed outcome $Y_i \in \mathcal{Y} \subseteq \mathbb{R}$. We assume the dataset \mathcal{D} are n i.i.d copies of the random variable $O = (X, A, Y) \sim p(O) = p(Y | X)p(A | X)p(X)$. In observational studies, the treatment assignment generally depends on the individuals' covariates, i.e., $A \not\perp\!\!\!\perp X$. This dependence is quantified via the conditional distribution $\pi(X) = p(A = 1 | X)$, also termed as the propensity score in the literature. To identify treatment effects, we make the following assumptions, which are standard in causal inference with observational studies [[Rosenbaum and Rubin, 1983](#)].

Assumption 1 (Consistency, Ignorability and Overlap). The observed outcome $Y_i = Y_i(A_i) = Y_i(a)$ if $A_i = a$, for $a \in \{0, 1\}$ and $i \in [n]$,² the distribution $p(O)$ satisfies strong ignorability: $Y(0), Y(1) \perp\!\!\!\perp A | X$ and overlap: $\exists \delta \in (0, 1)$ s.t. $\delta < p(A | X = x) < 1 - \delta, \forall x \in \mathcal{X}$.

We assume there exist two potential outcomes for each individual, the control outcome $Y(0)$ and the treated outcome $Y(1)$. The observed outcome is given by $Y = Y(A) = (1 - A)Y(0) + AY(1)$. For every individual in the dataset \mathcal{D} , we only get to observe one of the outcomes. With this, we can divide \mathcal{D} into a control set and a treated set, $\mathcal{D}_c = \{(X_i, A_i, Y_i) : i \in A_i = 0\}$ and $\mathcal{D}_t = \{(X_i, A_i, Y_i) : A_i = 1\}$. We denote the sample sizes of \mathcal{D}_c and \mathcal{D}_t by $n_c = |\mathcal{D}_c|$ and $n_t = |\mathcal{D}_t|$.

Under Assumption 1, we have $\mu_a(x) := \mathbb{E}\{Y(a) | X = x\} = \mathbb{E}\{Y | X = x, A = a\}$ for $a \in \{0, 1\}$. Then we can identify the conditional average treatment effect (CATE), i.e. the CATE function,

$$\tau(x) = \mathbb{E}[Y(1) - Y(0) | X = x] = \mu_1(x) - \mu_0(x),$$

from the data distribution $p(O)$. This identification formula motivates a common estimation strategy called a “T-learner”, where “T” refers to “Two” regression models. A T-learner estimates μ_0 and μ_1 by fitting two separate regression models, $\hat{\mu}_0$ and $\hat{\mu}_1$, on \mathcal{D}_c and \mathcal{D}_t , respectively. It estimates the CATE as the difference $\hat{\tau}(x) = \hat{\mu}_1(x) - \hat{\mu}_0(x)$. There are other advanced learners based on different identification formulas, e.g., X-learner [[Künzel et al., 2019](#)], R-learner [[Nie and Wager, 2021](#)] and DR-learner [[Kennedy, 2020](#)]. For example, the identification formula of a DR-learner is based on the (uncentered) first-order influence function ϕ of the ATE [[Hahn, 1998](#); [Robins and Rotnitzky, 1995](#)],

$$\tau(x) = \mathbb{E}\{\phi(X) | X = x\} = \mathbb{E}\left\{\frac{A}{\pi(x)}[Y - \mu_1(x)] + \mu_1(x) - \frac{1 - A}{1 - \pi(x)}[Y - \mu_0(x)] - \mu_0(x)\right\}.$$

Splitting \mathcal{D} into three subsets \mathcal{D}_1 , \mathcal{D}_2 and \mathcal{D}_3 , a DR-learner estimates the CATE as follows: estimate $\hat{\mu}_0$ and $\hat{\mu}_1$ on \mathcal{D}_1 , estimate $\hat{\pi}$ on \mathcal{D}_2 , then estimate $\hat{\tau}$ by regressing $\hat{\phi}(X)$ onto X in \mathcal{D}_3 , where $\hat{\phi}$ is obtained by estimating μ_0, μ_1 and π by the models $\hat{\mu}_0, \hat{\mu}_1$ and $\hat{\pi}$ in the expression of ϕ above. While these methods can be effective, the theory of nonparametric regression [[Stone, 1980](#)] demonstrates the presence of the dimensionality curse when estimating CATEs.

Definition 1 (Hölder ball). The Hölder ball $\mathcal{H}_d(s)$ is the set of functions $f : \mathbb{R}^d \rightarrow \mathbb{R}$ supported on $\mathcal{X} \subseteq \mathbb{R}^d$ with their partial derivatives satisfying that

$$\left| \frac{\partial^m f}{\partial^{m_1} \dots \partial^{m_d}}(x) - \frac{\partial^m f}{\partial^{m_1} \dots \partial^{m_d}}(x') \right| \lesssim \|x - x'\|_2^{s - \lfloor s \rfloor},$$

for all $x, x' \in \mathcal{X}$ and $m = (m_1, \dots, m_d)$ such that $\sum_{j=1}^d m_j = \lfloor s \rfloor$.

²The well-known *stable unit treatment value assumption* (SUTVA) assumes both no interference and consistency [[Rubin, 1980](#)]. The equation in our consistency assumption also implies no interference.

Formally, we assume μ_1, μ_0, π and τ are s -smooth functions in a Hölder ball $\mathcal{H}_d(s)$ for some non-negative smoothness parameter $s = \alpha_0, \alpha_1, \beta, \gamma$, respectively. Essentially, $\mathcal{H}_d(s)$ is the class of smooth functions that are close to their $\lfloor s \rfloor$ -order Taylor approximations.

Let $a \lesssim b$ denote the relation $a \leq Cb$ for some universal constant C . Suppose μ_0 and μ_1 are estimated with squared error $n_c^{-\frac{2\alpha_0}{2\alpha_0+d}}$ and $n_t^{-\frac{2\alpha_1}{2\alpha_1+d}}$. Using the inequality $(a+b)^2 \leq 2(a^2 + b^2)$, the expected risk of a T-learner is given by $\mathbb{E}\{[\tau(X) - \hat{\tau}(X)]^2\} \lesssim n_c^{-\frac{2\alpha_0}{2\alpha_0+d}} + n_t^{-\frac{2\alpha_1}{2\alpha_1+d}}$. Under mild assumptions, [Kennedy \[2020, Theorem 2\]](#) shows that a DR-learner's expected risk is given by

$$\begin{aligned} \mathbb{E}\{[\tau(X) - \hat{\tau}(X)]^2\} &\lesssim \mathbb{E}\{[\phi(X) - \hat{\phi}(X)]^2\} + \mathbb{E}\left\{[\pi(X) - \hat{\pi}(X)]^2 \sum_{a=0}^1 \{[\mu_a(X) - \hat{\mu}_a(X)]^2\}\right\} \\ &\leq \tilde{n}_3^{-\frac{2\gamma}{2\gamma+d}} + \tilde{n}_2^{-\frac{2\beta}{2\beta+d}} \left(\tilde{n}_{1,c}^{-\frac{2\alpha_0}{2\alpha_0+d}} + \tilde{n}_{1,t}^{-\frac{2\alpha_1}{2\alpha_1+d}} \right) \end{aligned}$$

where $\tilde{n}_m = |\mathcal{D}_m|$, $m = 1, 2, 3$, $\tilde{n}_{1,c}$ and $\tilde{n}_{1,t}$ are the amount of control and treated samples in \mathcal{D}_1 . While all of the discussed learners above are shown to be consistent, *they still suffer in finite samples*.

For doubly robust ATE estimators [\[Robins et al., 1994; Rotnitzky et al., 1998; Scharfstein et al., 1999\]](#), sample splitting is used to avoid making the Donsker class assumption on the models [\[Van der Vaart, 2000, Lemma 19.24\]](#). Cross-fitting (swap the split subsets, repeat the same procedure, and average the results) is often applied to regain full sample asymptotic efficiency [\[Robins et al., 2008; Chernozhukov et al., 2018\]](#). However, it remains unknown how much cross-fitting can help to remedy the damage from sample splitting to the finite sample risk bounds in the last equation; some analysis on aggregated models, e.g., [\[Yang, 2004\]](#), is needed to justify if an aggregated CATE estimator can improve the finite sample guarantee, i.e., the risk bound in the last equation.

Because of sample-splitting, it is difficult to conclude if a DR-learner can outperform a T-learner in finite samples. It is also unclear if we should use any of the simplified DR-learner variants proposed by [Curth and van der Schaar \[2021, Section 4\]](#), i.e. the RA- and PS-learner, even though neither are doubly robust. For example, a PS learner obtains $\hat{\phi}(\cdot)$ by estimating $\hat{\pi}(\cdot)$ on $\mathcal{D}_1 \cup \mathcal{D}_2$ and setting $\hat{\mu}_0(\cdot) = \hat{\mu}_1(\cdot) = 0$, then estimates $\hat{\tau}$ by regressing $\hat{\phi}(X)$ onto X on \mathcal{D}_3 . The risk bounds for these learners can be derived in a similar way as the last equation; see Theorem 1 in their paper. Both learners can have a better bound than the original DR-learner, depending on which of the outcome and propensity score models is smoother and if we use more samples on the smoother model.

For a \sqrt{n} -consistent estimator to exist, the requirement on the smoothness parameters is restrictive for moderate and large dimensions d , regardless of which learner we use. Furthermore, choosing the right learner to improve the situation is impossible without knowing the smoothness parameters. One way to make existing learners more suitable, is to reduce the curse of dimensionality before applying any CATE estimation. Reducing the dimensionality is feasible under the following assumption.

Assumption 2. For some positive integer $d^* < d$, there exist some variable $U \in \mathcal{U} \subseteq \mathbb{R}^{d^*}$ that generates the variables X, A and Y , i.e., the data distribution $p(O)$ satisfies that

$$p(O) = \int_{\mathcal{U}} p(Y \mid U = u)p(X \mid U = u)p(A \mid U = u)p(U = u) \, du.$$

The assumption is realistic generally as observational studies often collect covariates that represent the same aspect of an individual. For example, an individual's health status can be represented by some collection of covariates, e.g., blood pressure, temperature and some disease-specific symptoms. These covariates are correlated and contain overlapping information about the individual. The outcomes

and treatment assignment are dependent on these abstract aspects, rather than the covariates directly. Our goal is to learn these aspects as a low-dimensional representation of the covariates. We can then fit a model on the low dimensional representation, to estimate the outcomes and propensity score. The limitation of representation learning is that the representation itself is non-smooth. However, if a dataset is small, imbalanced and has a large number of covariates, the CATE function is too hard to estimate theoretically. Instead of feeding all the covariates into an ML model, we shall give consideration to representation learning, and use cross-validation on the observed outcomes to select the optimal dimension to work with. More importantly, the representation can be learnt using all the samples, i.e., both the treated and control group. Even more so, we may have access to much more unlabelled data in electronic health records besides our study. This is often the case because there is a time gap between the observation of covariates and the observation of the treatment and outcomes.

Instead of using any simple parametric models, we learn the latent representation with a neural network. This allows us to keep the nonparametric merit of the ML models built on top of the representation. Under Assumption 1, we consider the representation learning model, together with the outcome (propensity score) model, as an outcome (propensity score) model *based on the observed covariates*. The consistency of the resulting CATE estimator thus depends on the consistency of *both* models. This requires the representation to be identifiable, which is so far still impossible to achieve exactly for overparameterized neural networks. In our next section, we provide some approximate solution to this problem, sufficient for CATE estimation.

3 Model

A parameter is identifiable in a class of statistical models if every model describing the same distribution, has the same parameter-value across each model. If models with different parameters give the same data distribution, i.e., generate the same observed data in the large data limit, there is no guarantee we can find the true model from the data even if the sample size is large [Lewbel, 2019].

In our problem, the sought after representation is a continuous function, i.e., an infinite-dimensional parameter. Our goal is to construct partially identifiable representations in a class of energy-based models (EBMs). By partially identifiable, we mean if two EBMs model the same distribution, then the representation in the EBMs is the same up to some constant for all $x \in \mathcal{X}$. Generally, identifiability is often achieved by introducing some constraint on the model class, as is also the case here. We attain partial identifiability in two steps: (1) we create multiple EBMs with a shared representation, and (2) we fix some of the EBMs' parameters to a random value without overly reducing model complexity. We elaborate on these steps in detail below.

Step 1. Suppose we want to learn a k -dimensional representation of the covariates ($k < d$).³ We start by partitioning \mathcal{X} into some disjoint subsets $\mathcal{X}_1, \dots, \mathcal{X}_k$. Intuitively, with a partitioning of size k we want to create k equations to determine a k dimensional representation (for details, we refer to the proof of Proposition 2 below). The partition can not be random and should be made based on the value of a few (or all) covariates. In this paper, we construct the partition unsupervised by learning k -means clusters [Lloyd, 1982] from the covariates in the training data. Having a partition of size k , we now turn to representation learning.

³The risk bounds in Section 2 depend on the performance of the outcome and propensity score models. The dimension k can be tuned as a hyper-parameter via cross-validation on the observed outcomes (or treatment assignment) with an outcome regression (or propensity score) model. In this paper, we choose k only based on the observed outcomes because some CATE learners do not use a propensity score model.

Let $f_\theta : \mathcal{X} \rightarrow \mathbb{R}^k$ be a neural network, with which we define a standard EBM on each subset \mathcal{X}_j ,

$$p_{\theta,j}(x) = Z_{\theta,j}^{-1} \exp [-\beta_j^\top f_\theta(x)], \quad \forall j \in [k] \quad (1)$$

where the partition function $Z_{\theta,j} = \int_{\mathcal{X}_j} \exp [-\beta_j^\top f_\theta(x)] dx$ is finite and positive. The model in (1) can be written as an exponential family distribution,

$$p_{\theta,j}(x) = h(x) \exp [\lambda_j^\top f_\theta(x) - \psi_{\theta,j}],$$

where $h(x) = 1$ and $\lambda_j = -\beta_j$, and $\psi_{\theta,j} = \log \left(\int_{\mathcal{X}_j} h(x) \exp [\lambda_j^\top f_\theta(x)] dx \right)$.

Proposition 1. *For every $j \in [k]$, f_θ is a minimum and sufficient statistic in model (1).*

Step 2. Let $\mathcal{P} = \{p_{\theta,j} : \beta_j \in \mathbb{R}^k, \theta \in \Theta\}$ denote the space of EBMs defined in (1), and $\mathcal{P}(\beta_j)$ denote the subset of \mathcal{P} with β_j fixed. Let $B = (\beta_1, \dots, \beta_k)$ be the $k \times k$ matrix whose j -th column is β_j . In a standard EBM, both β_j and θ are learnable parameters. In a partially randomized EBM, we let B be a fixed random orthogonal matrix, such that θ is the only learnable parameter. One easy approach to construct B is to first generate a random matrix $B_0 \in \mathbb{R}^{k \times k}$, where each entry is drawn independently from a standard normal distribution, and then taking B as the matrix of eigenvectors in the eigendecomposition of B_0 . We move on to formally define a partially randomized EBM.

Definition 2 (Partially Randomized EBM). Given a partition of the covariates space, $\bigcup_{j=1}^k \mathcal{X}_j = \mathcal{X}$, a partially randomized EBM is given by $p_\theta = (p_{\theta,j} : j \in [k]) \in \bigtimes_{j=1}^k \mathcal{P}(\beta_j)$, where $B = (\beta_1, \dots, \beta_k)$ is a $k \times k$ random orthogonal matrix s.t. $BB^\top = I_{k \times k}$.

In a partially randomized EBM, we divide the covariates distribution $p(x)$ into k conditional distributions $p_j(x) = p(X = x | X \in \mathcal{X}_j)$. Next, we model each p_j using a standard EBM $p_{\theta,j}$ with fixed β_j . Importantly, our EBM achieves partial identifiability, which we define as follows:

Proposition 2. *For any $k \times k$ random orthogonal matrix B and $p_{\theta,j}, p_{\tilde{\theta},j} \in \mathcal{P}(\beta_j)$ such that $p_{\theta,j}(\cdot) = p_{\tilde{\theta},j}(\cdot)$ for every $j \in [k]$, we have*

$$f_\theta(\cdot) - f_{\tilde{\theta}}(\cdot) = C \quad \text{for some constant vector } C = C(\theta, \tilde{\theta}). \quad (2)$$

Perhaps surprisingly, the modelling strategy above does not overly decrease the model complexity. Proposition 3 verifies the universal approximation capability of the partially randomized EBM. The proof is attained by showing that $\mathcal{P}(\beta_j)$ satisfies the conditions in the Stone-Weierstrass theorem when f_θ is a simple neural network. The proofs of all the propositions can be found in Appendix A.

Proposition 3. *For any continuous density function $p : \mathcal{X} \rightarrow \mathbb{R}^+$, $k \times k$ random orthogonal matrix B , and $\epsilon > 0$, there exists $p_{\theta,j} \in \mathcal{P}(\beta_j)$ such that $\sup_{x \in \mathcal{X}} |p_j(x) - p_{\theta,j}(x)| \leq \epsilon$ for all $j \in [k]$.*

Next, we will show that training the partially randomized EBM with a noise contrastive loss function will converge to some consistent set of limits whose representations are only different by a universal constant. This is sufficient for the regression models to remain consistent because a model is indifferent to conditioning on a random variable, or the same random variable plus some constant. Furthermore, by standardizing the learnt representations, we can fix their mean to 0 and their variance to 1 in any sample size. Given that the representations have mean 0 and variance 1, by partial identifiability and consistency, the representations obtained from different runs of the experiments will have a correlation close to 1 at each dimension in large samples, as is demonstrated in Section 6.2.

4 Method

Fitting energy-based models (EBMs) by maximum likelihood estimation (MLE) is often infeasible because the partition function ($Z_{\theta,j}$) is intractable. Noise Contrastive Estimation (NCE) proposed by [Gutmann and Hyvärinen \[2010, 2012\]](#) is a computationally efficient and a consistent alternative. The high-level idea of NCE is to optimize an EBM by contrasting it with another noise distribution with known and easy-to-sample density. Advanced methods have been proposed to tune the noise distribution, see for example [Gao et al. \[2020\]](#); [Bose et al. \[2018\]](#) and [Ceylan and Gutmann \[2018\]](#).

Here we divide the n individuals into subsets $\mathcal{I}_j = \{i \in [n] : X_i \in \mathcal{X}_j\}$, $j \in [k]$. For every individual $i \in \mathcal{I}_j$, we draw b corrupted samples $\tilde{X}_{i1}, \dots, \tilde{X}_{ib}$ from a distribution $\tilde{p}_j(x)$ defined as follows. Each \tilde{X}_{ia} is generated in two steps: (1) we sample an independent binary variable with some probability for each feature of X_i , used to decide which features of X_i will be corrupted, then (2) corrupt each selected continuous feature by adding white noise drawn from a standard normal distribution, and corrupt each selected categorical feature by uniformly sampling a possible value from its range.

For every individual $i \in \mathcal{I}_j$, we have $\tilde{X}_i = (X_i, \tilde{X}_{i1}, \dots, \tilde{X}_{ib}) \sim p_j(x_i) \prod_{a=1}^b \tilde{p}_j(\tilde{x}_{ia})$, where $p_j(x) = p(X = x \mid X \in \mathcal{X}_j)$. Suppose we randomly permute the columns of \tilde{X}_i and let $V_i = (V_{i,1}, \dots, V_{i,b+1})$ be the permuted \tilde{X}_i . Each column of V_i has equal probability $\frac{1}{b+1}$ for being the clean sample X_i . Let $W_i \in \{0, 1\}^{b+1}$ indicate which column of V_i is X_i . We can treat $\{(V_i, W_i) : i \in \mathcal{I}_j\}$ as a set of labeled ‘‘images’’ and optimize the EBM by solving a classification task. The predictive probability of $V_{i,a} = X_i$ is given by the posterior distribution,

$$q_{\theta,j}(a \mid V_i) = \frac{(b+1)^{-1} p_{\theta,j}(V_{i,a}) \prod_{a \in [b+1]: a' \neq a} \tilde{p}_j(V_{i,a'})}{\sum_{c=1}^{b+1} (b+1)^{-1} p_{\theta,j}(V_{i,c}) \prod_{c' \in [b+1]: c' \neq c} \tilde{p}_j(V_{i,c'})} = \frac{p_{\theta,j}(V_{i,a}) / \tilde{p}_j(V_{i,a})}{\sum_{c=1}^{b+1} p_{\theta,j}(V_{i,c}) / \tilde{p}_j(V_{i,c})}.$$

We estimate θ by maximizing the negative cross-entropy⁴, $\mathcal{L}_n(\theta) = k^{-1} \sum_{j=1}^k \mathcal{L}_{n,j}(\theta)$, where,

$$\mathcal{L}_{n,j}(\theta) = n_j^{-1} \sum_{i \in \mathcal{I}_j} \sum_{a=1}^{b+1} W_{ia} \log q_{\theta,j}(a \mid V_i) = n_j^{-1} \sum_{i \in \mathcal{I}_j} \log \frac{\sigma_{\theta,j}(X_i)}{\sigma_{\theta,j}(X_i) + \sum_{a=1}^b \sigma_{\theta,j}(\tilde{X}_{ia})}, \quad (3)$$

with $n_j = |\mathcal{I}_j|$ and $\sigma_{\theta,j}(\cdot) = \exp[\beta_j^\top f_\theta(\cdot) - \log \tilde{p}_j(\cdot)]$. The network f_θ is trained using all the samples in $\mathcal{L}_n(\theta)$, even though we split the samples into subsets.

Proposition 4. *Suppose that the covariates space \mathcal{X} is a compact subset of \mathbb{R}^d , $f_\theta(x)$ has a compact parameter space Θ , and $f_\theta(x)$ is continuous with respect to its parameter θ for any $x \in \mathcal{X}$. For any $k \times k$ random orthogonal matrix $B = (\beta_1, \dots, \beta_k)$ and partition $\bigcup_{j=1}^k \mathcal{X}_j = \mathcal{X}$, under Proposition 3, we assume for any continuous density function $p(x)$ defined on \mathcal{X} , these exists a countable subset $\Theta_0 \subset \Theta$ s.t. $p_{\theta_0,j}(x) = p_j(x)$ for any $x \in \mathcal{X}_j$, $j \in [k]$ and $\theta_0 \in \Theta_0$. For any positive integer b and $\hat{\theta}_n \in \arg \max_{\theta \in \Theta} \mathcal{L}_n(\theta)$, we have $\lim_{n \rightarrow \infty} \hat{\theta}_n \in \Theta_0$ with probability 1.*

Proposition 4 shows that the estimate $\hat{\theta}_n$ based on $\mathcal{L}_n(\theta)$ can only converge to a set of limits Θ_0 . This is mainly due to the partially identifiability discussed in the last section. Nevertheless, the representations given by f_{θ_0} are different by some universal constant for all $\theta_0 \in \Theta_0$. Essentially, both MLE and NCE are special cases of M-estimators in statistics [[Van der Vaart, 2000](#)]. The proposition is proven by showing that $\mathcal{L}_{\infty,j}(\theta)$ is maximized by $q_{\theta,j}(a \mid V_i)$ with $p_{\theta,j} = p_j$, and the

⁴This is also called the ranking objective in the literature of NCE [[Józefowicz et al., 2016](#); [Ma and Collins, 2018](#)]. Here we reformulate the objective function as a more intuitive multiclass classification task.

standard conditions for consistent M-estimators hold for the estimate $\hat{\theta}_n$ under a weaker identifiability assumption; see Appendix A.4 for more details.

Ceylan and Gutmann [2018, Section 2] shows that if every \tilde{X}_{ia} is given by adding some noise to X_i , the NCE objective is approximately equal to the score matching (SM) objective [Hyvärinen, 2005]. [Swersky et al., 2011] shows that applying SM to Gaussian EBMs is corresponding to training a particular form of a regularized autoencoder. Similarly, Vincent [2011] finds that denoising score matching (DSM) can be related to the denoising autoencoder (DAE) training criterion in [Vincent et al., 2010]. Roughly speaking, all these methods follow the same principle: assuming the covariates are structural, i.e., live in some d^* -dimensional manifold ($d^* < d$), to distinguish or reconstruct true samples from their noisy proxies, the models need to learn a low-dimensional representation that captures the data structure i.e., the shape of the data manifold.

5 Related works

The models and learners developed for CATE estimation (Sections 1 and 2) and contrastive learning (Section 4) have been discussed above. Here we provide more related works on two different areas.

Identifiability theory. Khemakhem et al. [2020b] propose two definitions of identifiability for EBMs; weak and strong identifiability (in their Definitions 1 and 2). Their EBM is more complex than ours with β_j as a learnable parameter, while their objective is to identify both β_j and $f_\theta(x)$. This is unnecessary for the application in our paper. Arguably, the partial identifiability defined in our paper is stronger than both of their definitions. In their strong identifiability, each dimension of f_θ is identifiable up to be multiplied by and plus some constant, and each dimension of f_θ can be permuted in any order. They also require a specific neural network architecture for f_θ . In our work, we use a *simpler* partially randomized EBM to achieve a *stricter* version of identifiability, without sacrificing the approximation capability of the EBM or restricting the architecture of f_θ .

The works on nonlinear ICA and its generalization [Hyvarinen and Morioka, 2016; Hyvarinen et al., 2019; Khemakhem et al., 2020a] are the first to propose the idea of using contrastive learning for identifiable feature extraction when some auxiliary information (e.g., time steps) about the features is available. We use sample-splitting and a noise contrastive loss function for training the partially randomized EBM, assuming *no auxiliary information* is provided in the observational data. [Monti et al., 2020; Wu and Fukumizu, 2020] propose non-linear ICA based methods for causal inference on structural causal models [Pearl, 2009]. The setup and problems studied in their papers are different from our method which is developed within the potential outcomes framework.

Representation learning. Representation learning is recently applied to balance or match the covariate distribution between the treated and control group in observational studies, by minimizing the distributional distance between the group [Shalit et al., 2017], preserving local similarity [Yao et al., 2018], minimizing counterfactual variance [Zhang et al., 2020] and adversarial training [Kallus, 2020]. We note that supervised dimensionality reduction in a deep learning model is not reliable because the model can easily overfit the limited outcome data without finding an informative representation of the covariates. Our proposed method works more generally as a preprocessing step to reduce the dimensionality curse for any ML model and learner in CATE estimation, including these deep learning models which balance the distribution in one of their hidden layers.

In statistics, sufficient dimensionality reduction (SDR) [Lee et al., 2013; Cook, 2009; Li, 1991; Adragni and Cook, 2009] has been used in the models for estimating ATE and CATE [Huang and Yang, 2020; Luo et al., 2019; Cheng et al., 2020; Ma et al., 2019; Ghosh et al., 2018]. If the subspace spanned by

the columns of a $d \times k$ matrix θ with $k \leq d$ satisfies that $Y \perp\!\!\!\perp X \mid \theta^\top X$, we call this subspace an SDR subspace. The idea of SDR is to project the covariates X onto this subspace before feeding it into a parametric or nonparametric regression model to estimate Y . To achieve the desired conditional independence, θ is jointly learnt with the regression model. This is not straightforward for some of the ML models. e.g., decision tree. [Kallus et al. \[2018\]](#) proposes a matrix factorization based method for preprocessing noisy and missing covariates. In contrast with these methods, our method performs nonlinear dimensionality reduction of the covariates, which is more general and effective for the data living in some low-dimensional manifold, including linear subspace. [Nabi and Shpitser \[2017\]](#) and [Berrevoets et al. \[2020\]](#) propose methods to deal with high-dimensional treatment variables, e.g., radiation and organ exposure, which is not the problem we consider in this paper.

6 Experiments

We make two claims in our paper: (1) by using our method as a preprocessing step, one can increase the performance of any CATE-learner; (2) our method remains partially identifiable, which is an important property for the continued consistency of the downstream-CATE learner. We test these two claims in the following subsections. Throughout our experiments we use four different CATE learners: an X-Learner, a DR-learner, a T-Learner, and an R-learner [[Microsoft Research, 2019](#)]. We provide more details on our experiments (e.g., on learners and hyperparameters) in Appendix B.

6.1 CATE estimation

Our main contribution is a way to increase performance for *any* learner. Specifically, in high dimensions and small sample sizes. We evaluate learners' performance using *precision of estimating heterogeneous effects* (PEHE) introduced in [Hill \[2011\]](#) and now standard in CATE estimation. PEHE is essentially the expected risk $\mathbb{E}\{[\hat{\tau}(X) - \tau(X)]^2\}$ we define in Section 2. Because an individual's treated and control outcomes are never observed jointly, the CATE function is unobserved in any real-world dataset. The literature thus relies on (semi-)synthetic data to properly evaluate CATE-learners.

In our synthetic setup, the generating process of the observed variables $O = (X, A, Y)$ starts by sampling a latent variable $U \sim \mathcal{N}(0, I_{5 \times 5})$. Then we generate a set of covariates $X = \mathcal{N}(g(U), I_{d \times d})$, two potential outcomes, $\mu_0(U)$ and $\mu_1(U)$ and a treatment assignment $A \sim \pi(U)$. The observed outcome is given by $Y = \mathcal{N}(A\mu_0(U) + (1 - A)\mu_1(U), 1)$. The CATE function is given by $\tau(U) = \mu_1(U) - \mu_0(U)$. The function g is a deep ReLU neural network; μ_0 and μ_1 are one-layer neural networks, with an exp-function on their output layers; π is a one-layer network with a sigmoid-function on its output layer. By generating i.i.d samples from this process, we create a training set (with size n specified in Table 1) and a large testing set with 20k samples.

Given a training set, we first use it to optimize the EBM. Then we preprocess the same training set and apply a variety of CATE learners on these lower-dimensional representations. As a comparison, we also apply the same CATE learners on the original covariates.

Table 1 shows that our method greatly benefits a broad spectrum of CATE learners on the synthetic dataset and semi-synthetic dataset Twins [[Almond et al., 2005](#)] with real covariates, especially in small sample sizes. While the gain of using our method diminishes somewhat in larger sample sizes, it is still significant. More importantly, we observe that with EBM, the performance gaps between different learners shrink significantly. Specifically, R-learner with EBM has the best performance on average over the table while it performs poorly in small samples without EBM. Overall, the

Table 1: **Results on synthetic data and semi-synthetic data (Twins).** Each row reports the average PEHE (lower is better) over ten runs for each CATE learner (standard deviation in scriptsize): both *with* representations (indicated as “✓”), and *without* representation (indicated as “✗”). For each run, we learn a new representation. In the above two blocks, we vary sample sizes and dimensions using our synthetic setup, and in the bottom block we vary the sample size for the Twins-dataset. Using our EBM yields superior testing performance for a range of CATE learners (indicated in bold). In green, we emphasize the best models per row, each time *with* EBM. While there may be duplicate values in this table, we highlight only those that are best beyond the rounding applied here.

Methods		X-Learner		DR-Learner		T-Learner		R-Learner	
EBM		✗	✓	✗	✓	✗	✓	✗	✓
<i>d</i>		<i>Synth.</i> data with increasing sample size and increasing dimensions							
50	100	2.309 ±.00	1.994 ±.02	4.594 ±.56	2.017 ±.04	2.441 ±.00	1.993 ±.01	3.194 ±.26	1.982 ±.04
100	250	2.779 ±.00	2.018 ±.01	4.056 ±.32	2.154 ±.39	2.838 ±.00	2.019 ±.01	3.702 ±.23	2.018 ±.01
150	500	2.618 ±.00	2.000 ±.01	3.030 ±.12	2.001 ±.01	2.641 ±.00	2.000 ±.01	2.877 ±.08	2.000 ±.01
200	1k	2.185 ±.00	1.940 ±.01	2.283 ±.02	1.941 ±.01	2.189 ±.00	1.939 ±.01	2.271 ±.01	1.940 ±.01
250	1.5k	2.267 ±.00	1.949 ±.02	2.427 ±.01	1.976 ±.00	2.271 ±.00	1.948 ±.01	2.436 ±.02	1.949 ±.02
<i>n</i>		<i>Synth.</i> data with increasing sample size and dimensions fixed at <i>d</i> = 100							
100		2.134 ±.00	1.927 ±.01	24.61 ±9.9	2.096 ±.09	2.279 ±.00	1.929 ±.01	3.192 ±.13	1.925 ±.01
250		2.779 ±.00	2.018 ±.01	4.056 ±.32	2.154 ±.39	2.838 ±.00	2.019 ±.01	3.702 ±.23	2.018 ±.01
500		2.155 ±.00	2.056 ±.02	2.334 ±.07	2.273 ±.67	2.166 ±.00	2.053 ±.02	2.271 ±.05	2.056 ±.02
1k		2.059 ±.00	1.964 ±.02	2.105 ±.01	2.016 ±.16	2.061 ±.00	1.964 ±.02	2.086 ±.01	1.965 ±.02
1.5k		2.013 ±.00	1.998 ±.02	2.043 ±.01	1.998 ±.02	2.014 ±.00	1.998 ±.02	2.024 ±.01	1.991 ±.02
<i>n</i>		Twins (<i>d</i> = 48) with increasing sample size							
500		0.214 ±.00	0.144 ±.00	0.236 ±.04	0.182 ±.05	0.221 ±.00	0.145 ±.00	0.222 ±.02	0.145 ±.00
1k		0.294 ±.00	0.162 ±.00	0.348 ±.12	0.173 ±.03	0.301 ±.00	0.162 ±.01	0.532 ±.11	0.161 ±.00
1.5k		0.165 ±.00	0.154 ±.00	0.189 ±.06	0.159 ±.01	0.165 ±.00	0.154 ±.00	0.172 ±.01	0.154 ±.00
2k		0.167 ±.00	0.156 ±.00	0.197 ±.03	0.159 ±.00	0.167 ±.00	0.156 ±.00	0.222 ±.05	0.157 ±.00
2.5k		0.297 ±.00	0.153 ±.00	0.390 ±.19	0.156 ±.00	0.297 ±.00	0.153 ±.00	0.358 ±.22	0.153 ±.00

experiment results align with our theoretical discussion in Section 2: (1) There is no consensus on the best learner in finite samples; (2) by reducing the dimensionality d to a smaller number, the upper bounds of the expected risk (i.e., the finite sample difference between the learners) will decrease faster as the sample size increases. To further validate our proposed method, we repeat the same experiment using additional dimensionality reduction methods, additional ML models and data, and report consistent results to those we present in this section, in Appendix B.

6.2 Partial identifiability of representations

In this section we dive deeper, and shed light on the identifiability of our method. Having an identifiable method is important for later inspection of the representations, but also to decrease the standard deviation of CATE learners. The latter is especially important in practice.

The leftmost panel in Figure 1 reports the standard deviation of an R-learner when fitted on: an autoencoder (AE) and our method (EBM). Each representation is fitted to the same amount of dimensions (reported as a hyperparameter in Appendix B). The result shows that our model decreases

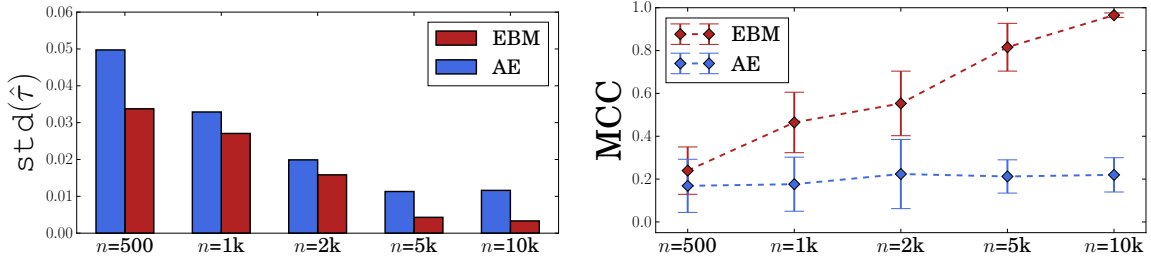


Figure 1: **Results on identifiability.** *Left*—For each model (an autoencoder (AE), and our model (EBM)) we learn ten distinct representations. We then fit an R-Learner on each representation, and calculate the standard deviation of their CATE estimates. Our method has lower standard errors compared to AE. *Right*—We report the mean correlation coefficient (MCC) between the representations on the Twins data (higher is better). Our EBM becomes more consistent with larger samples (error bars indicate standard deviation on MCC), and even tends to 1 in large samples.

the standard deviation across various sample sizes—an important quality in practice, as many applications require estimates to be consistent. As discussed at the end of Section 4, the learnt representations after standardization should correlate as sample size increases. We train our EBM for ten times using distinct random initializations, while keeping the random matrix fixed across runs. We subsequently compute the mean correlation coefficient (MCC) between the representations of the test-set from different runs. The mean correlation is computed by averaging the correlation between *each dimension* in the representations of 20k samples from the test set. Note that the latter is a strict definition as it requires the representation to be consistent for each *individual* dimension.⁵ Reported in the rightmost panel, we see that our EBM’s MCC grows as the sample size increases, leaving the (unidentifiable) AE behind, indicating that our EBM is indeed identifiable.

7 Discussion

We propose a partially randomized EBM with universal approximation capability to learn a partially identifiable low-dimensional representation of moderate to high-dimensional covariates in CATE estimation. We show theoretically and empirically that our representations converge to a set differing only by some constant. This is sufficient for the downstream ML model and learner to achieve consistency when estimating CATEs. Experiments on multiple datasets with various dimensions and sample sizes have demonstrated a performance increase when using our method for CATE estimation.

Our work opens a few new directions for future research. First, our method currently operates within the standard setup of observational studies in causal inference, while our partial identifiability theory does not rely on the network architecture of f_θ . Extending our work to other high-dimensional settings such as time series or vision could prove useful for many real world applications. Second, as an interpretable approach within CATE estimation, matching is concerned with finding similar individuals across treatment and control groups. While effective, matching becomes harder in high-dimensions. Extending our approach to remain interpretable (e.g. by measuring each covariate’s influence to each dimension in the representation) can arm matching approaches against the dimensionality curse. In essence, we believe our method could benefit a wide range of applications requiring causal inference.

⁵Previous work [Khemakhem et al., 2020b] tests identifiability using the MCC maximized by canonical-correlation analysis (CCA). Here we compute the exact correlation to test our stronger version of identifiability.

References

Kofi P Adragni and R Dennis Cook. Sufficient dimension reduction and prediction in regression. *Philosophical Transactions of the Royal Society A: Mathematical, Physical and Engineering Sciences*, 367(1906):4385–4405, 2009.

Ahmed M. Alaa and Mihaela van der Schaar. Bayesian inference of individualized treatment effects using multi-task gaussian processes. In *NIPS*, 2017.

Douglas Almond, Kenneth Y Chay, and David S Lee. The costs of low birth weight. *The Quarterly Journal of Economics*, 120(3):1031–1083, 2005.

Sanjeev Arora, Nadav Cohen, and Elad Hazan. On the optimization of deep networks: Implicit acceleration by overparameterization. In *International Conference on Machine Learning*, pages 244–253. PMLR, 2018.

Peter L Bartlett, Andrea Montanari, and Alexander Rakhlin. Deep learning: a statistical viewpoint. *arXiv preprint arXiv:2103.09177*, 2021.

Jeroen Berrevoets, James Jordon, Ioana Bica, Alexander Gimson, and Mihaela van der Schaar. OrganITE: Optimal transplant donor organ offering using an individual treatment effect. In *Advances in Neural Information Processing Systems*, volume 33, pages 20037–20050. Curran Associates, Inc., 2020.

Lukas Biewald. Experiment tracking with weights and biases, 2020. URL <https://www.wandb.com/>. Software available from wandb.com.

Avishhek Joey Bose, Huan Ling, and Yanshuai Cao. Adversarial contrastive estimation. *arXiv preprint arXiv:1805.03642*, 2018.

Ciwan Ceylan and M. Gutmann. Conditional noise-contrastive estimation of unnormalised models. In *ICML*, 2018.

Debo Cheng, Jiuyong Li, Lin Liu, and Jixue Liu. Sufficient dimension reduction for average causal effect estimation. *arXiv preprint arXiv:2009.06444*, 2020.

Victor Chernozhukov, Denis Chetverikov, Mert Demirer, Esther Duflo, Christian Hansen, Whitney Newey, and James Robins. Double/debiased machine learning for treatment and structural parameters, 2018.

R Dennis Cook. *Regression graphics: Ideas for studying regressions through graphics*, volume 482. John Wiley & Sons, 2009.

Alicia Curth and Mihaela van der Schaar. Nonparametric estimation of heterogeneous treatment effects: From theory to learning algorithms. In *International Conference on Artificial Intelligence and Statistics*, pages 1810–1818. PMLR, 2021.

Gerald B Folland. *Real analysis: modern techniques and their applications*, volume 40. John Wiley & Sons, 1999.

Dylan J Foster and Vasilis Syrgkanis. Orthogonal statistical learning. *arXiv preprint arXiv:1901.09036*, 2019.

Ruiqi Gao, Erik Nijkamp, Diederik P Kingma, Zhen Xu, Andrew M Dai, and Ying Nian Wu. Flow contrastive estimation of energy-based models. In *Proceedings of the IEEE/CVF Conference on Computer Vision and Pattern Recognition*, pages 7518–7528, 2020.

Trinetri Ghosh, Yanyuan Ma, and Xavier de Luna. Sufficient dimension reduction for feasible and robust estimation of average causal effect. *arXiv preprint arXiv:1811.01992*, 2018.

Michael Gutmann and Aapo Hyvärinen. Noise-contrastive estimation: A new estimation principle for unnormalized statistical models. In *Proceedings of the Thirteenth International Conference on Artificial Intelligence and Statistics*, pages 297–304. JMLR Workshop and Conference Proceedings, 2010.

Michael U Gutmann and Aapo Hyvärinen. Noise-contrastive estimation of unnormalized statistical models, with applications to natural image statistics. *Journal of Machine Learning Research*, 13(2), 2012.

Jinyong Hahn. On the role of the propensity score in efficient semiparametric estimation of average treatment effects. *Econometrica*, pages 315–331, 1998.

P Richard Hahn, Jared S Murray, Carlos M Carvalho, et al. Bayesian regression tree models for causal inference: Regularization, confounding, and heterogeneous effects (with discussion). *Bayesian Analysis*, 15(3):965–1056, 2020.

Jennifer L Hill. Bayesian nonparametric modeling for causal inference. *Journal of Computational and Graphical Statistics*, 20(1):217–240, 2011.

Ming-Yueh Huang and S. Yang. Robust inference of conditional average treatment effects using dimension reduction. *arXiv: Methodology*, 2020.

A. Hyvärinen. Estimation of non-normalized statistical models by score matching. *J. Mach. Learn. Res.*, 6:695–709, 2005.

Aapo Hyvarinen and Hiroshi Morioka. Unsupervised feature extraction by time-contrastive learning and nonlinear ica. *arXiv preprint arXiv:1605.06336*, 2016.

Aapo Hyvarinen, Hiroaki Sasaki, and Richard Turner. Nonlinear ica using auxiliary variables and generalized contrastive learning. In *The 22nd International Conference on Artificial Intelligence and Statistics*, pages 859–868. PMLR, 2019.

Robert I Jennrich. Asymptotic properties of non-linear least squares estimators. *The Annals of Mathematical Statistics*, 40(2):633–643, 1969.

R. Józefowicz, Oriol Vinyals, M. Schuster, Noam M. Shazeer, and Y. Wu. Exploring the limits of language modeling. *ArXiv*, abs/1602.02410, 2016.

Nathan Kallus. Deepmatch: Balancing deep covariate representations for causal inference using adversarial training. In *International Conference on Machine Learning*, pages 5067–5077. PMLR, 2020.

Nathan Kallus, Xiaojie Mao, and Madeleine Udell. Causal inference with noisy and missing covariates via matrix factorization. *arXiv preprint arXiv:1806.00811*, 2018.

Edward H Kennedy. Optimal doubly robust estimation of heterogeneous causal effects. *arXiv preprint arXiv:2004.14497*, 2020.

Ilyes Khemakhem, Diederik Kingma, Ricardo Monti, and Aapo Hyvarinen. Variational autoencoders and nonlinear ica: A unifying framework. In *International Conference on Artificial Intelligence and Statistics*, pages 2207–2217. PMLR, 2020a.

Ilyes Khemakhem, Ricardo Monti, Diederik Kingma, and Aapo Hyvarinen. Ice-beem: Identifiable conditional energy-based deep models based on nonlinear ica. *Advances in Neural Information Processing Systems*, 33, 2020b.

Sören R Künzel, Jasjeet S Sekhon, Peter J Bickel, and Bin Yu. Metalearners for estimating heterogeneous treatment effects using machine learning. *Proceedings of the national academy of sciences*, 116(10):4156–4165, 2019.

Kuang-Yao Lee, Bing Li, Francesca Chiaromonte, et al. A general theory for nonlinear sufficient dimension reduction: Formulation and estimation. *Annals of Statistics*, 41(1):221–249, 2013.

Arthur Lewbel. The identification zoo: Meanings of identification in econometrics. *Journal of Economic Literature*, 57(4):835–903, 2019.

Ker-Chau Li. Sliced inverse regression for dimension reduction. *Journal of the American Statistical Association*, 86(414):316–327, 1991.

Stuart Lloyd. Least squares quantization in pcm. *IEEE transactions on information theory*, 28(2):129–137, 1982.

Wei Luo, Wenbo Wu, and Yeying Zhu. Learning heterogeneity in causal inference using sufficient dimension reduction. *Journal of Causal Inference*, 7(1), 2019.

Shujie Ma, Liping Zhu, Zhiwei Zhang, Chih-Ling Tsai, and Raymond J Carroll. A robust and efficient approach to causal inference based on sparse sufficient dimension reduction. *Annals of statistics*, 47(3):1505, 2019.

Zhuang Ma and Michael Collins. Noise contrastive estimation and negative sampling for conditional models: Consistency and statistical efficiency. *ArXiv*, abs/1809.01812, 2018.

Marian F MacDorman and Jonnae O Atkinson. Infant mortality statistics from the 1997 period linked birth/infant death data set. 1999.

Microsoft Research. EconML: A Python Package for ML-Based Heterogeneous Treatment Effects Estimation. <https://github.com/microsoft/EconML>, 2019. Version 0.11.1.

Ricardo Pio Monti, Kun Zhang, and Aapo Hyvärinen. Causal discovery with general non-linear relationships using non-linear ica. In *Uncertainty in Artificial Intelligence*, pages 186–195. PMLR, 2020.

Razieh Nabi and I. Shpitser. Semi-parametric causal sufficient dimension reduction of high dimensional treatments. *arXiv: Methodology*, 2017.

Whitney K Newey and Daniel McFadden. Large sample estimation and hypothesis testing. *Handbook of econometrics*, 4:2111–2245, 1994.

Jersey Neyman. Sur les applications de la théorie des probabilités aux expériences agricoles: Essai des principes. *Roczniki Nauk Rolniczych*, 10:1–51, 1923.

Xinkun Nie and Stefan Wager. Quasi-oracle estimation of heterogeneous treatment effects. *Biometrika*, 108(2):299–319, 2021.

Judea Pearl. *Causality*. Cambridge university press, 2009.

F. Pedregosa, G. Varoquaux, A. Gramfort, V. Michel, B. Thirion, O. Grisel, M. Blondel, P. Prettenhofer, R. Weiss, V. Dubourg, J. Vanderplas, A. Passos, D. Cournapeau, M. Brucher, M. Perrot, and E. Duchesnay. Scikit-learn: Machine learning in Python. *Journal of Machine Learning Research*, 12:2825–2830, 2011.

D. Pollard. Strong consistency of k -means clustering. *Annals of Statistics*, 9:135–140, 1981.

James Robins, Lingling Li, Eric Tchetgen, Aad van der Vaart, et al. Higher order influence functions and minimax estimation of nonlinear functionals. In *Probability and statistics: essays in honor of David A. Freedman*, pages 335–421. Institute of Mathematical Statistics, 2008.

James M Robins and Andrea Rotnitzky. Semiparametric efficiency in multivariate regression models with missing data. *Journal of the American Statistical Association*, 90(429):122–129, 1995.

James M Robins, Andrea Rotnitzky, and Lue Ping Zhao. Estimation of regression coefficients when some regressors are not always observed. *Journal of the American statistical Association*, 89(427):846–866, 1994.

Paul R Rosenbaum and Donald B Rubin. The central role of the propensity score in observational studies for causal effects. *Biometrika*, 70(1):41–55, 1983.

Paul R Rosenbaum and Donald B Rubin. Reducing bias in observational studies using subclassification on the propensity score. *Journal of the American statistical Association*, 79(387):516–524, 1984.

Paul R Rosenbaum and Donald B Rubin. Constructing a control group using multivariate matched sampling methods that incorporate the propensity score. *The American Statistician*, 39(1):33–38, 1985.

Andrea Rotnitzky, James M Robins, and Daniel O Scharfstein. Semiparametric regression for repeated outcomes with nonignorable nonresponse. *Journal of the american statistical association*, 93(444):1321–1339, 1998.

Donald B Rubin. Estimating causal effects of treatments in randomized and nonrandomized studies. *Journal of educational Psychology*, 66(5):688, 1974.

Donald B. Rubin. Comment on "randomization analysis of experimental data: The fisher randomization test". *Journal of the American Statistical Association*, 75(371):591, 1980. doi: 10.2307/2287653. URL <https://doi.org/10.2307/2287653>.

Daniel O Scharfstein, Andrea Rotnitzky, and James M Robins. Adjusting for nonignorable drop-out using semiparametric nonresponse models. *Journal of the American Statistical Association*, 94(448):1096–1120, 1999.

Uri Shalit, Fredrik D Johansson, and David Sontag. Estimating individual treatment effect: generalization bounds and algorithms. In *International Conference on Machine Learning*, pages 3076–3085. PMLR, 2017.

Charles J Stone. Optimal rates of convergence for nonparametric estimators. *The annals of Statistics*, pages 1348–1360, 1980.

Kevin Swersky, Marc’Aurelio Ranzato, David Buchman, Benjamin M Marlin, and Nando de Freitas. On autoencoders and score matching for energy based models. In *ICML*, 2011.

Aad W Van der Vaart. *Asymptotic statistics*, volume 3. Cambridge university press, 2000.

Pascal Vincent. A connection between score matching and denoising autoencoders. *Neural computation*, 23(7):1661–1674, 2011.

Pascal Vincent, H. Larochelle, Isabelle Lajoie, Yoshua Bengio, and Pierre-Antoine Manzagol. Stacked denoising autoencoders: Learning useful representations in a deep network with a local denoising criterion. *J. Mach. Learn. Res.*, 11:3371–3408, 2010.

Stefan Wager and Susan Athey. Estimation and inference of heterogeneous treatment effects using random forests. *Journal of the American Statistical Association*, 113(523):1228–1242, 2018.

Jeffrey M Wooldridge. *Econometric analysis of cross section and panel data*. MIT press, 2010.

Pengzhou Wu and Kenji Fukumizu. Causal mosaic: Cause-effect inference via nonlinear ica and ensemble method. In *International Conference on Artificial Intelligence and Statistics*, pages 1157–1167. PMLR, 2020.

Y. Yang. Aggregating regression procedures to improve performance. *Bernoulli*, 10:25–47, 2004.

Liuyi Yao, Sheng Li, Yaliang Li, Mengdi Huai, Jing Gao, and Aidong Zhang. Representation learning for treatment effect estimation from observational data. *Advances in Neural Information Processing Systems*, 31, 2018.

In-Kwon Yeo and Richard A Johnson. A new family of power transformations to improve normality or symmetry. *Biometrika*, 87(4):954–959, 2000.

Jinsung Yoon, James Jordon, and Mihaela van der Schaar. Ganite: Estimation of individualized treatment effects using generative adversarial nets. In *International Conference on Learning Representations*, 2018.

Yao Zhang, Alexis Bellot, and Mihaela van der Schaar. Learning overlapping representations for the estimation of individualized treatment effects. *ArXiv*, abs/2001.04754, 2020.

A Proofs

A.1 Proof of Proposition 1

Proof. The sufficiency of f_θ is obtained immediately by applying Fisher–Neyman factorization theorem to (1). Consider another sufficient statistics $\tilde{u} : \mathcal{X}_j \rightarrow \mathcal{U}$. By the factorization theorem, we can factorize the distribution as $p_{\theta,j}(x) = \tilde{h}(x)\tilde{g}(\tilde{u}(x), \beta_j)$ for some functions \tilde{h} and \tilde{g} . Given any x and x' such that $u(x) = u(x')$, i.e., $\tilde{g}(\tilde{u}(x), \beta_j) = \tilde{g}(\tilde{u}(x'), \beta_j)$, we have

$$\exp[-\beta_j^\top (f_\theta(x) - f_\theta(x'))] = \frac{p_{\theta,j}(x)}{p_{\theta,j}(x')} = \frac{\tilde{h}(x)}{\tilde{h}(x')}.$$

The first equality uses two facts of the EBM: (1) $h(x)$ is constant ($h(x) = 1$), and (2) $Z_{\theta,j}$ is for fixed β_j . The ratio on the right-hand side does not depend on β_j , which holds if and only if $f_\theta(x) = f_\theta(x')$. That is, for any sufficient statistics u and any x, x' , $u(x) = u(x')$ implies that $f_\theta(x) = f_\theta(x')$ and hence that $f_\theta(x)$ is a function of $u(x)$. Then f_θ is a minimal sufficient statistic. \square

A.2 Proof of Proposition 2

Proof. Consider two different parameter values θ and $\tilde{\theta}$ such that $p_{\theta,j}(x) = p_{\tilde{\theta},j}(x)$. Using the expression (1) and applying logarithm to both sides,

$$\beta_j^\top f_\theta(x) = \beta_j^\top f_{\tilde{\theta}}(x) + \log \frac{Z_{\theta,j}}{Z_{\tilde{\theta},j}}. \quad (4)$$

By concatenating the last equation for all $j \in [k]$, we have

$$B^\top f_\theta(x) = B^\top f_{\tilde{\theta}}(x) + G \quad (5)$$

where $G = (\log \frac{Z_{\theta,j}}{Z_{\tilde{\theta},j}} : j \in [k])$ is a k -dimensional vector. By definition, $BB^\top = I_{k \times k}$. Then multiplying the two side of (5) by B gives (2). \square

Any invertible matrix B can be used to attain the partial identifiability. However, the orthogonal matrix is a simple sufficient condition that allows us to prove the universal approximation capability of the partially randomized EBM (Proposition 3); see the proof of the proposition in Appendix A.3.

A.3 Proof of Proposition 3

Theorem 1 (Stone-Weierstrass; Theorem 4.45 in [Folland \[1999\]](#)). *Suppose $\mathcal{X} = [0, 1]^d$, and that \mathcal{P} is a class of functions satisfying the following conditions:*

- (i) *Every $p \in \mathcal{P}$ is continuous.*
- (ii) *For every $x \in \mathcal{X}$, there exist $p \in \mathcal{P}$ such that $p(x) \neq 0$.*
- (iii) *For every $x, x' \in \mathcal{X}$ such that $x \neq x'$, there exist $p \in \mathcal{P}$ such that $p(x) \neq p(x')$.*
- (iv) *\mathcal{F} is closed under multiplication and under vector space operations.*

Then for every continuous density function $g : \mathcal{X} \rightarrow \mathbb{R}^+$ and $\epsilon > 0$, there exist $p \in \mathcal{P}$ s.t.

$$\sup_{x \in \mathcal{X}} |g(x) - p(x)| \leq \epsilon.$$

The original Stone-Weierstrass theorem works for any $g : \mathcal{X} \rightarrow \mathbb{R}$. Here we modify the codomain of g to be \mathbb{R}^+ because we only consider estimating density functions. We note Stone-Weierstrass theorem works for any $\mathcal{X} \subseteq \mathbb{R}^d$. Choosing $\mathcal{X} = [0, 1]^d$ is common practice in the literature of approximation theory and nonparametric regression. It is used to simplify the notation in the proof. The proof idea holds trivially for general $\mathcal{X} \subseteq \mathbb{R}^d$.

Proof. Suppose f_θ is a linear neural network in the model (1), we have

$$p_{\theta, j} \in \mathcal{P}(\beta_j) := \left\{ x \rightarrow Z_{\theta, j}^{-1} \exp [-\beta_j^\top \theta x] : \theta \in \mathbb{R}^{k \times d} \right\}$$

The first condition in Theorem 1 is satisfied directly by definition. If θ is a zero matrix, then $p_{\theta, j}(x) \neq 0$, which means the second condition in Theorem 1 holds. Given any $x_1, x_2 \in \mathcal{X}_j$ such that $x_1 \neq x_2$, we can always find a exponential function along the line between x_1 and x_2 . Because the exponential function $p_{\theta, j} \in \mathcal{P}(\beta_j)$ is nonlinear, we have $p_{\theta, j}(x_1) \neq p_{\theta, j}(x_2)$. Formally, we let $\theta = -\left(\sum_{j'=1}^k \beta_{j'}\right)(x_1 - x_2)^\top$, then

$$-\beta_j^\top \theta = 1 \cdot (x_1 - x_2)^\top = (x_1 - x_2)^\top,$$

The first equality uses the fact that β_j is a unit vector in the random orthogonal matrix B . Then,

$$p_{\theta, j}(x) = Z_{\theta, j}^{-1} \exp [(x_1 - x_2)^\top x].$$

Because $x_1 \neq x_2$, we have

$$\frac{p_{\theta, j}(x_1)}{p_{\theta, j}(x_2)} = \frac{\exp [x_1^\top x_1 - x_2^\top x_1]}{\exp [x_1^\top x_2 - x_2^\top x_2]} = \exp [-(x_1 - x_2)^\top (x_1 - x_2)] > 0,$$

which proves that the third condition in Theorem 1 holds. The space $\mathcal{P}(\beta_j)$ is closed under vector space operations by definition. It is also closed under multiplication. By the property of exponential functions, $\exp [-\beta_j^\top \theta x_1] \cdot \exp [-\beta_j^\top \theta x_2] = \exp [-\beta_j^\top \theta(x_1 + x_2)]$, it is straightforward to show that given some functions p 's $\in \mathcal{P}(\beta_j)$, the multiplication of two different linear combinations of p 's is still in the span of p 's. Thus, $\mathcal{P}(\beta_j)$ satisfies the fourth condition in Theorem 1. \square

Although the derivation is based on a linear network f_θ for simplicity, it does not mean we should use a linear network in practice. In recent years, it has been shown theoretically and empirically that overparametrization in deep neural networks allows gradient methods to find interpolating solutions; these methods implicitly impose regularization; overparametrization leads to benign overfitting, that is, accurate predictions (i.e., better generalization) despite overfitting training data; overparametrization also accelerates the stochastic optimization of neural networks [Arora et al., 2018]; see [Bartlett et al., 2021] for a review of the theoretical analysis on overparameterized models.

A.4 Proof of Proposition 4

Proof. As discussed in the main paper, both MLE and NCE are M-estimators. The consistency proof of M-estimators is hardly new. Here we apply the existing proof techniques to verify the convergence

of contrastive learning in optimizing our special energy-based model under the partial identifiability assumption. The proof consists of two steps: (1) we show $q_{\theta,j}(a \mid V_i)$ with $p_{\theta,j} = p_j$ is a maximizer of $\mathcal{L}_{\infty,j}(\theta)$, then (2) we show the standard conditions of consistent M-estimators hold for $\mathcal{L}_n(\theta)$. Under a different formulation of multiclass classification, the first step follows the proof idea of [Ma and Collins, 2018, Theorem 3.2]. The second step is essentially the proof of [Wooldridge, 2010, Theorem 12.2] and [Newey and McFadden, 1994, Theorem 2.5] under a weaker identifiability assumption. The compactness assumptions on \mathcal{X} and Θ are needed in the second step for applying the uniform law of large numbers [Jennrich, 1969, Theorem 2] on $\mathcal{L}_n(\theta)$.

Step 1. Recall that for every $i \in \mathcal{I}_j$, we have $\bar{X}_i = (X_i, \tilde{X}_{i1}, \dots, \tilde{X}_{ib}) \sim p_j(x_i) \prod_{a=1}^b \tilde{p}_j(\tilde{x}_{ia})$, where $p_j(x) = p(X = x \mid X \in \mathcal{X}_j)$. We randomly permute the columns of \bar{X}_i and let $V_i = (V_{i,1}, \dots, V_{i,b+1})$ be the permuted \bar{X}_i . Each column of V_i has equal probability $\frac{1}{b+1}$ for being the clean sample X_i . Let $W_i \in \{0, 1\}^{b+1}$ indicate which column of V_i is X_i . Here, we define a categorical variable $S_i \in [b+1]$ such that $S_i = a$ if $W_{ia} = 1$. Then, we have

$$p(S_i = a) = \frac{1}{b+1}, \quad \forall a \in [b+1].$$

Because $\tilde{X}_{i1}, \dots, \tilde{X}_{ib}$ are drawn from the sample distribution \tilde{p}_j , their order in the permutation does not matter for their joint distribution. The we define the marginal distribution as

$$\begin{aligned} \Lambda_j(V_i) &= \sum_{a=1}^{b+1} p(S_i = a) p(V_i \mid S_i = a) \\ &= \sum_{a=1}^{b+1} (b+1)^{-1} p_j(V_{i,a}) \prod_{a' \in [b+1]: a' \neq a} \tilde{p}_j(V_{i,a'}) \\ &= \sum_{a=1}^{b+1} (b+1)^{-1} \frac{p_j(V_{i,a})}{\tilde{p}_j(V_{i,a})} \prod_{a' \in [b+1]} \tilde{p}_j(V_{i,a'}). \end{aligned}$$

Then the distribution of V_i conditional on $S_i = a$ is given by

$$\begin{aligned} p(V_i \mid S_i = a) &= p_j(V_{i,a}) \prod_{a' \in [b+1]: a' \neq a} \tilde{p}_j(V_{i,a'}) \\ &= \frac{p_j(V_{i,a})}{\tilde{p}_j(V_{i,a})} \prod_{a' \in [b+1]} \tilde{p}_j(V_{i,a'}) \\ &= (b+1)^{-1} p_j(V_{i,a}) / \tilde{p}_j(V_{i,a}) \prod_{a' \in [b+1]} \tilde{p}_j(V_{i,a'}) \cdot (b+1) \frac{\Lambda_j(V_i)}{\Lambda_j(V_i)} \\ &= \frac{(b+1)^{-1} p_j(V_{i,a}) / \tilde{p}_j(V_{i,a}) \prod_{a' \in [b+1]} \tilde{p}_j(V_{i,a'})}{\sum_{c=1}^{b+1} (b+1)^{-1} p_j(V_{i,c}) / \tilde{p}_j(V_{i,c}) \prod_{a' \in [b+1]} \tilde{p}_j(V_{i,a'})} \cdot (b+1) \Lambda_j(V_i) \\ &= \frac{(b+1)^{-1} p_j(V_{i,a}) / \tilde{p}_j(V_{i,a})}{\sum_{c=1}^{b+1} (b+1)^{-1} p_j(V_{i,c}) / \tilde{p}_j(V_{i,c})} \cdot (b+1) \Lambda_j(V_i) \\ &= (b+1) \Lambda_j(V_i) p_j(a \mid V_i). \end{aligned}$$

where $p_j(a \mid V_i)$ is the predictive probability of $S_i = a$ based on the true distribution p_j ,

$$p_j(a \mid V_i) = \frac{p_j(V_{i,a}) / \tilde{p}_j(V_{i,a})}{\sum_{c=1}^{b+1} p_j(V_{i,c}) / \tilde{p}_j(V_{i,c})}$$

As $n \rightarrow \infty$, i.e., $n_j \rightarrow \infty$, the objective function in (3) is given by

$$\begin{aligned}\mathcal{L}_{\infty,j}(\theta) &= \sum_{a=1}^{b+1} p(S_i = a) \int p_j(v \mid S_i = a) \log q_{\theta,j}(a \mid v) dv \\ &= \frac{1}{b+1} \sum_{a=1}^{b+1} \int (b+1) \Lambda_j(v) p_j(a \mid v) \log q_{\theta,j}(a \mid v) dv \\ &= \int \Lambda_j(v) \left[\sum_{a=1}^{b+1} p_j(a \mid v) \log q_{\theta,j}(a \mid v) \right] dv\end{aligned}$$

Because $\Lambda_j(v) > 0$ and Lemma 1, $\mathcal{L}_{\infty,j}(\theta)$ is maximized when

$$q_{\theta,j}(a \mid v) = p_j(a \mid v), \quad \forall a \in [b+1]. \quad (6)$$

Then, suppose $v_{a'} = v^*$ for all $a' \in [b+1] \setminus \{a\}$, we continue to write (6) as

$$\begin{aligned}\frac{p_{\theta,j}(v_a)/\tilde{p}_j(v_a)}{\sum_{c=1}^{b+1} p_{\theta,j}(v_c)/\tilde{p}_j(v_c)} &= \frac{p_j(v_a)/\tilde{p}_j(v_a)}{\sum_{c=1}^{b+1} p_j(v_c)/\tilde{p}_j(v_c)} \\ \frac{p_{\theta,j}(v_a)}{\sum_{c=1}^{b+1} p_{\theta,j}(v_c)/\tilde{p}_j(v_c)} &= \frac{p_j(v_a)}{\sum_{c=1}^{b+1} p_j(v_c)/\tilde{p}_j(v_c)} \\ \frac{\sum_{c=1}^{b+1} p_{\theta,j}(v_c)/\tilde{p}_j(v_c)}{p_{\theta,j}(v_a)} &= \frac{\sum_{c=1}^{b+1} p_j(v_c)/\tilde{p}_j(v_c)}{p_j(v_a)} \\ \sum_{c \neq a} \frac{p_{\theta,j}(v_c)}{\tilde{p}_j(v_c)p_{\theta,j}(v_a)} &= \sum_{c \neq a} \frac{p_j(v_c)}{\tilde{p}_j(v_c)p_j(v_a)} \\ \frac{p_{\theta,j}(v^*)}{p_{\theta,j}(v_a)} &= \frac{p_j(v^*)}{p_j(v_a)} \\ \beta_j^\top [f_\theta(v^*) - f_\theta(v_a)] &= \beta_j^\top [f_{\theta_0}(v^*) - f_{\theta_0}(v_a)],\end{aligned}$$

where $\theta_0 \in \Theta_0$. Combing the last equation for all $j \in [k]$ and using the fact that B is a orthogonal matrix, we have

$$\begin{aligned}B^\top [f_\theta(v^*) - f_\theta(v_a)] &= B^\top [f_{\theta_0}(v^*) - f_{\theta_0}(v_a)] \\ f_\theta(v^*) - f_\theta(v_a) &= f_{\theta_0}(v^*) - f_{\theta_0}(v_a) \\ f_\theta(v_a) &= f_{\theta_0}(v_a) + c(\theta, \theta_0)\end{aligned}$$

Then, we have

$$p_{\theta,j}(x) = Z_{\theta,j}^{-1} \exp [-\beta_j^\top f_\theta(x)] = \frac{\exp [-\beta_j^\top f_{\theta_0}(x) - \beta_j^\top c(\theta, \theta_0)]}{\int_{\mathcal{X}_j} \exp [-\beta_j^\top f_{\theta_0}(x) - \beta_j^\top c(\theta, \theta_0)] dx} = p_j(x).$$

For any $\hat{\theta} \in \arg \max_{\theta \in \Theta} \mathcal{L}_{\infty,j}(\theta)$, we have $p_{\hat{\theta},j}(x) = p_j(x)$ for any $x \in \mathcal{X}_j$.

Step 2. Because \mathcal{X} and Θ are compact, the value of each covariate and network parameter is bounded. Then the function we optimize in Equation (3),

$$g_j(\bar{x}; \theta) = \log \frac{\sigma_{\theta,j}(x)}{\sigma_{\theta,j}(x_i) + \sum_{a=1}^b \sigma_{\theta,j}(\tilde{x}_{ia})}$$

is bounded for any $\bar{x} = (x, \tilde{x}_{i1}, \dots, \tilde{x}_{ib})$. Let $\mathbb{E}_n [g_j(\bar{X}; \theta)] = n_j^{-1} \sum_{i \in \mathcal{I}_j} g_j(\bar{X}_i; \theta)$. Using the uniform law of large number (ULLN) (see [Jenrich, 1969, Theorem 2] and [Newey and McFadden, 1994, Lemma 2.4]), we have

$$\sup_{\theta \in \Theta} |\mathbb{E}_n [g_j(\bar{X}; \theta)] - \mathbb{E} [g_j(\bar{X}; \theta)]| \xrightarrow{P} 0.$$

Now we change the exact identifiability assumption in [Wooldridge, 2010, Theorem 12.2] and [Newey and McFadden, 1994, Theorem 2.5] to our partial identifiability assumption. Suppose there is a countable subset $\Theta_0 \subset \Theta$ such that for every $\theta_0 \in \Theta_0$, $p_{\theta_0, j}$ gives the same distribution as p_j , and any θ_0 is a non-unique maximizer of $\mathbb{E} [g_j(\bar{X}; \theta)]$. Suppose we define a open ball with radius equal to $\eta > 0$ for every $\theta_0 \in \Theta_0$. The region inside and outside these open balls is given by

$$\Theta_\eta = \left\{ \theta \in \Theta \mid \arg \min_{\theta_0 \in \Theta_0} \|\theta - \theta_0\|_2 < \eta \right\} \quad \text{and} \quad \Theta_\eta^c = \left\{ \theta \in \Theta \mid \arg \min_{\theta_0 \in \Theta_0} \|\theta - \theta_0\|_2 \geq \eta \right\}.$$

Using the proof of [Newey and McFadden, 1994, Theorem 2.1], for any $\epsilon > 0$, $\theta_0 \in \Theta_0$ and $\hat{\theta} \in \arg \max \mathbb{E}_n [g_j(\bar{X}; \theta)]$, we have with probability approaching to 1:

$$\mathbb{E} [g_j(\bar{X}; \hat{\theta})] > \mathbb{E} [g_j(\bar{X}; \theta_0)] - \epsilon. \quad (7)$$

By the compactness of Θ_η^c and the assumption that f_θ is continuous w.r.t to θ , we have

$$\sup_{\theta \in \Theta_\eta^c} \mathbb{E} [g_j(\bar{X}; \theta)] = \mathbb{E} [g_j(\bar{X}; \theta^*)] < \mathbb{E} [g_j(\bar{X}; \theta_0)] \quad \text{for some } \theta^* \in \Theta_\eta^c.$$

Thus, by choosing

$$\epsilon = \mathbb{E} [g_j(\bar{X}; \theta_0)] - \sup_{\theta \in \Theta_\eta^c} \mathbb{E} [g_j(\bar{X}; \theta)],$$

it follows from (7) that with probability approaching to 1,

$$\mathbb{E} [g_j(\bar{X}; \hat{\theta})] > \sup_{\theta \in \Theta_\eta^c} \mathbb{E} [g_j(\bar{X}; \theta)] \Rightarrow \hat{\theta} \in \Theta_\eta. \quad (8)$$

Since (8) is true for any $\eta > 0$, we have $\hat{\theta} \in \Theta_0$ with probability 1 as $n_j \rightarrow \infty$. We note that the same proof holds if we consider the summation of $\mathbb{E}_n [g_j(\bar{X}; \theta)]$ over all $j \in [k]$. Therefore, we prove the main claim in the proposition that for any positive integer b and $\hat{\theta}_n \in \arg \max_{\theta \in \Theta} \mathcal{L}_n(\theta)$, we have $\lim_{n \rightarrow \infty} \hat{\theta}_n \in \Theta_0$ with probability 1. Finally, in practice we partition \mathcal{X} into $\mathcal{X}_1, \dots, \mathcal{X}_k$ by applying the k -means clustering algorithm [Lloyd, 1982] on the training data. The proof presented here is still valid given the strong consistency of k -means clustering [Pollard, 1981]. \square

Lemma 1. Suppose $w = (w_1, \dots, w_b) > 0$ and $\sum_{a=1}^b w_a = 1$,

$$f(\tilde{w}; w) = \sum_{a=1}^b w_a \log \tilde{w}_a \quad \text{subject to} \quad \tilde{w} = (\tilde{w}_1, \dots, \tilde{w}_b) > 0 \quad \text{and} \quad \sum_{a=1}^b \tilde{w}_a = 1.$$

Then $f(\tilde{w}; w)$ is maximized at $\tilde{w} = w$.

Proof. Suppose

$$g(\tilde{w}; w) = \sum_{a=1}^b w_a \log \tilde{w}_a + \lambda \left(\sum_{a=1}^b \tilde{w}_a - 1 \right).$$

We have

$$\frac{\partial g(\tilde{w}; w)}{\partial \tilde{w}_c} = 0 \Rightarrow \lambda = -\frac{w_c}{\tilde{w}_c}.$$

and

$$\frac{\partial g(\tilde{w}; w)}{\partial \lambda} = 0 \Rightarrow \sum_{a=1}^b \tilde{w}_a = 1.$$

Combining both conditions, we have

$$\sum_{a=1}^b \tilde{w}_a = -\frac{1}{\lambda} \sum_{a=1}^b w_a = -\frac{1}{\lambda} = 1 \Rightarrow \lambda = -1.$$

Then, $-1 = -\frac{w_c}{\tilde{w}_c} \Rightarrow \tilde{w}_c = w_c$. By a second-derivative test on the bordered Hessian of $g(\tilde{w}; w)$, we have $\tilde{w} = (\tilde{w}_1, \dots, \tilde{w}_b) = (w_1, \dots, w_b)$ is a maximizer of the function $f(\tilde{w}; w)$. \square

B Additional experiments & Hyperparameters

In Appendix B.1 we compare a variety of dimensionality reduction methods to our EBM, by using each as a preprocessing step before constructing a CATE estimator. In Appendix B.2 we repeat our experiments in Table 1 using different regression models to estimate the outcomes and propensity score in the same CATE learners, and using an additional real-world dataset. For hyperparameter settings we refer to Appendix B.3, and for details on used CATE learners we refer to Appendix B.4.

B.1 Comparision to alternative dimensionality reduction methods

In Table 2 we compare our EBM to a variety of alternative dimensionality reduction methods. Specifically, we compare against: principal components analysis (PCA), Feature Agglomeration (FA), Spectral Embedding (SE), Isomap, KernelPCA with an RBF kernel, and Autoencoder (AE). From Table 2 we note that none of these methods succeeds in successfully learning informative representations, in such a way to keep downstream CATE learners accurate; our EBM outperforms the benchmarks in most cases over different datasets with various dimensions and sample sizes.

B.2 CATE learners with different regression models, and different data

Consider Tables 3-4-5, where we report the PEHE given the same experimental setup as we have in Table 1; for additional data (Infant Health Development Program (IHDP) [MacDorman and Atkinson, 1999]), and three additional regression models (PowerTransform Regression [Yeo and Johnson, 2000], Polynomial Regression, and Ridge Regression, respectively). From our results we learn that our EBM is agnostic to the choice of regression model, and is versatile enough to also perform well given other data. These results are promising and should give some assurance regarding our method before application in practice. As we have in Table 1, we ran each CATE learner on ten distinct representations, given different folds of the data, and averaged the results. Note that we have not specifically optimised the EBM’s hyperparameters for these different regression models, but rather kept them as they were in Table 1 (actual hyperparameter values are reported in Table 7). We also include a “complete” version of Table 1 in Table 6, where we include results on IHDP as an additional dataset. Note that these results are in line with those reported earlier using different regression models, as well as our results reported in the main text.

Table 2: **Results using different dimensionality reduction techniques.** Using an R-learner, we report the PEHE of our EBM and other benchmark techniques: PCA, Feature Agglomeration (FA), Spectral Embedding (SE), Isomap, and KernelPCA (K-PCA) and Autoencoder (AE).

Methods	PCA	FA	SE	Isomap	K-PCA	AE	EBM
<i>d n Synth. data with increasing sample size and increasing dimensions</i>							
50 100	2.139 ±.00	2.123 ±.00	2.183 ±.00	2.135 ±.00	2.141 ±.00	2.259 ±.02	1.982 ±.01
100 250	2.238 ±.00	2.239 ±.00	2.151 ±.00	2.231 ±.00	2.236 ±.00	2.055 ±.01	2.032 ±.01
150 500	2.224 ±.00	2.209 ±.00	2.963 ±.00	2.231 ±.00	2.239 ±.00	2.092 ±.03	2.034 ±.02
200 1k	2.152 ±.00	2.154 ±.00	2.097 ±.00	2.168 ±.00	2.168 ±.00	1.995 ±.02	1.945 ±.01
250 1.5k	2.158 ±.01	2.163 ±.00	2.401 ±.00	2.229 ±.00	2.196 ±.00	2.071 ±.05	1.962 ±.02
<i>n Synth. data with increasing sample size and dimensions fixed at d = 100</i>							
100	2.194 ±.03	2.203 ±.04	2.262 ±.00	2.156 ±.01	2.127 ±.00	2.476 ±.18	1.955 ±.03
250	2.238 ±.00	2.244 ±.01	2.150 ±.00	2.233 ±.01	2.232 ±.00	2.109 ±.02	2.032 ±.01
500	2.119 ±.01	2.029 ±.01	2.395 ±.00	2.230 ±.00	2.118 ±.00	2.092 ±.04	2.008 ±.00
1k	2.183 ±.00	2.231 ±.00	2.145 ±.00	2.219 ±.00	2.199 ±.00	2.059 ±.01	1.987 ±.02
1.5k	2.174 ±.00	2.213 ±.00	2.083 ±.00	2.229 ±.00	2.199 ±.00	2.048 ±.01	2.007 ±.01
<i>n Twins (d = 48) with increasing sample size</i>							
500	1.092 ±.11	1.758 ±.1.1	1.011 ±.00	1.006 ±.00	1.015 ±.00	0.580 ±.03	0.163 ±.00
1k	1.015 ±.00	0.963 ±.00	1.010 ±.00	1.004 ±.00	1.010 ±.00	0.549 ±.04	0.153 ±.00
1.5k	1.014 ±.00	0.965 ±.00	1.005 ±.00	1.006 ±.00	1.012 ±.00	0.546 ±.04	0.153 ±.00
2k	1.013 ±.00	0.957 ±.00	1.009 ±.00	1.007 ±.00	1.013 ±.00	0.579 ±.03	0.159 ±.00
2.5k	1.007 ±.00	0.951 ±.00	1.002 ±.00	1.006 ±.00	1.006 ±.00	0.542 ±.04	0.161 ±.00
<i>n IHDP (d = 25) with increasing sample size</i>							
100	6.266 ±.34	1.833 ±.02	5.295 ±.00	5.276 ±.02	5.448 ±.04	3.580 ±.1.2	2.444 ±.73
250	6.243 ±.06	1.624 ±.04	5.180 ±.00	6.145 ±.07	5.564 ±.02	2.811 ±.73	1.729 ±.19
500	6.995 ±.05	1.951 ±.01	5.293 ±.00	5.988 ±.06	6.469 ±.15	2.671 ±.14	1.635 ±.09

Table 3: **Results on (semi)-synthetic data (Twins & IHDP) with PowerTransform Regression.** We report for the same configuration as in Table 1. Results are averaged over ten runs with (“✓”), and without (“✗”) the same representations used in Table 1.

Methods	X-Learner		DR-Learner		T-Learner		R-Learner	
EBM	✗	✓	✗	✓	✗	✓	✗	✓
<i>d n Synth. data with increasing sample size and increasing dimensions</i>								
50 100	2.267 ±.00	2.010 ±.03	5.593 ±2.2	2.015 ±.05	2.455 ±.00	2.011 ±.03	53.17 ±5.2	11.16 ±3.9
100 250	2.754 ±.00	2.019 ±.01	3.963 ±.24	2.027 ±1.2	2.798 ±.00	2.020 ±.01	60.10 ±4.2	10.70 ±3.9
150 500	2.575 ±.00	2.002 ±.01	2.986 ±.08	2.001 ±.01	2.595 ±.00	2.001 ±.01	49.78 ±4.2	12.31 ±1.8
200 1k	2.197 ±.00	1.952 ±.00	2.293 ±.03	1.941 ±.01	2.202 ±.00	1.951 ±.01	42.76 ±3.9	2.838 ±.64
250 1.5k	2.288 ±.00	1.966 ±.04	2.410 ±.04	1.979 ±.03	2.295 ±.00	1.968 ±.04	42.03 ±3.6	2.535 ±.15
<i>n Synth. data with increasing sample size and dimensions fixed at d = 100</i>								
100	2.150 ±.00	1.964 ±.02	32.63 ±13	2.147 ±.15	2.289 ±.00	1.973 ±.03	58.80 ±5.1	5.713 ±2.2
250	2.754 ±.00	2.019 ±.01	3.963 ±.24	2.027 ±1.2	2.798 ±.00	2.020 ±.01	60.10 ±4.2	10.70 ±3.9
500	2.150 ±.00	2.029 ±.02	2.319 ±.06	2.006 ±.05	2.160 ±.00	2.028 ±.03	41.85 ±3.4	3.884 ±.79
1k	2.053 ±.00	1.986 ±.02	2.102 ±.01	1.989 ±.01	2.057 ±.00	1.987 ±.02	39.49 ±3.2	2.637 ±.20
1.5k	2.008 ±.00	1.999 ±.02	2.354 ±.01	1.999 ±.52	2.008 ±.00	2.000 ±.02	37.17 ±2.9	3.949 ±.77
<i>n Twins (d = 48) with increasing sample size</i>								
500	0.203 ±.00	0.187 ±.06	4.383 ±.22	0.185 ±.02	0.204 ±.00	0.248 ±.24	300.0 ±16.	2.176 ±.89
1k	0.177 ±.00	0.169 ±.03	0.194 ±.01	0.163 ±.01	0.177 ±.00	0.159 ±.02	31.39 ±2.5	1.029 ±1.1
1.5k	0.169 ±.00	0.154 ±.00	0.172 ±.01	0.183 ±.08	0.169 ±.00	0.155 ±.00	31.23 ±2.3	0.459 ±.15
2k	0.167 ±.00	0.161 ±.00	0.168 ±.00	0.163 ±.00	0.168 ±.00	0.161 ±.00	29.95 ±2.4	0.629 ±.30
2.5k	0.169 ±.00	0.162 ±.00	0.170 ±.00	0.163 ±.00	0.169 ±.00	0.162 ±.00	29.79 ±2.4	0.439 ±.19
<i>n IHDP (d = 25) with increasing sample size</i>								
100	1.814 ±.01	1.502 ±.03	3.755 ±.72	1.637 ±.12	1.845 ±.00	1.507 ±.05	35.77 ±6.3	21.36 ±17.
250	1.713 ±.00	1.598 ±.04	1.837 ±.09	1.653 ±.13	1.727 ±.00	1.593 ±.03	11.71 ±1.5	9.552 ±4.0
500	1.603 ±.00	1.554 ±.02	1.672 ±.05	1.571 ±.03	1.627 ±.00	1.556 ±.02	23.45 ±2.5	15.19 ±3.9

Table 4: **Results on (semi-)synthetic data (Twins & IHDP) using Polynomial Regression.** We report for the same configuration as in Table 1. Results are averaged over ten runs with (“✓”), and without (“✗”) the same representations used in Table 1.

Methods		X-Learner		DR-Learner		T-Learner		R-Learner	
EBM		✗	✓	✗	✓	✗	✓	✗	✓
<i>d</i>									
<i>n</i>									
<i>Synth. data with increasing sample size and increasing dimensions</i>									
50	100	2.095 ±.00	2.089 ±.09	75.12 ±26.	2.500 ±.44	2.124 ±.00	2.095 ±.09	110.8 ±7.1	26.61 ±7.6
100	250	2.109 ±.00	2.026 ±.03	11.67 ±1.9	2.138 ±.30	2.168 ±.00	2.028 ±.03	50.45 ±4.4	10.72 ±4.0
150	500	2.048 ±.00	2.008 ±.02	8.668 ±1.5	2.006 ±.01	2.142 ±.00	2.008 ±.02	44.29 ±3.4	12.35 ±1.8
200	1k	1.964 ±.00	1.949 ±.02	7.278 ±1.3	1.949 ±.02	2.088 ±.00	1.949 ±.02	42.04 ±3.4	2.973 ±.57
250	1.5k	1.945 ±.00	1.945 ±.03	6.764 ±1.2	1.979 ±.03	2.109 ±.00	1.945 ±.04	41.71 ±3.5	2.555 ±.18
<i>n</i>									
<i>Synth. data with increasing sample size and dimensions fixed at d = 100</i>									
100		2.009 ±.00	1.987 ±.09	157.1 ±50.	2.176 ±.13	2.038 ±.00	1.992 ±.09	54.81 ±4.3	6.612 ±3.5
250		2.109 ±.00	2.019 ±.01	11.67 ±1.9	2.028 ±.02	2.168 ±.00	2.019 ±.01	50.46 ±4.4	9.623 ±3.0
500		1.897 ±.00	2.055 ±.05	8.020 ±1.7	2.003 ±.00	2.007 ±.00	2.051 ±.05	43.56 ±3.9	3.758 ±.82
1k		2.210 ±.00	1.995 ±.02	5.871 ±.90	2.289 ±.88	2.338 ±1.4	1.996 ±.02	40.38 ±3.1	2.965 ±.69
1.5k		2.341 ±.00	2.002 ±.02	4.637 ±.75	2.156 ±.47	2.474 ±.00	2.000 ±.02	38.31 ±2.9	3.945 ±.76
<i>n</i>									
<i>Twins (d = 48) with increasing sample size</i>									
500		0.345 ±.00	0.155 ±.00	4.538 ±1.4	0.158 ±.00	0.377 ±.00	0.155 ±.00	116.0 ±14.	0.847 ±.19
1k		0.486 ±.00	0.149 ±.00	1.747 ±.33	0.157 ±.01	0.529 ±.00	0.149 ±.00	78.22 ±7.3	0.482 ±.11
1.5k		0.455 ±.00	0.153 ±.00	1.453 ±.40	0.186 ±.06	0.481 ±.00	0.153 ±.00	142.3 ±21.	0.395 ±.13
2k		0.426 ±.00	0.159 ±.00	1.109 ±.32	0.162 ±.00	0.451 ±.00	0.159 ±.00	38.13 ±4.2	0.655 ±.33
2.5k		0.403 ±.00	0.159 ±.00	0.921 ±.14	0.163 ±.01	0.418 ±.00	0.159 ±.00	33.39 ±2.8	0.459 ±.19
<i>n</i>									
<i>IHDP (d = 25) with increasing sample size</i>									
100		1.608 ±.02	1.565 ±.25	8.076 ±2.4	1.956 ±.64	1.944 ±.00	1.542 ±.18	24.53 ±5.1	11.52 ±8.4
250		2.335 ±.00	1.637 ±.02	8.607 ±.82	1.964 ±.49	2.219 ±.00	1.627 ±.03	35.37 ±3.8	18.13 ±7.8
500		2.177 ±.00	1.536 ±.00	4.216 ±.35	1.739 ±.36	2.233 ±.00	1.535 ±.00	26.06 ±4.5	10.18 ±5.6

Table 5: **Results on (semi-)synthetic data (Twins & IHDP) with Ridge Regression.** We report for the same configuration as in Table 1. Results are averaged over ten runs with (“✓”), and without (“✗”) the same representations used in Table 1.

Methods		X-Learner		DR-Learner		T-Learner		R-Learner	
EBM		✗	✓	✗	✓	✗	✓	✗	✓
<i>d</i>									
<i>n</i>									
<i>Synth. data with increasing sample size and increasing dimensions</i>									
50	100	2.373 ±.00	2.001 ±.02	10.53 ±4.8	2.028 ±.06	2.471 ±.00	1.997 ±.02	53.24 ±5.3	11.33 ±3.9
100	250	2.802 ±.00	2.021 ±.01	8.769 ±1.5	2.041 ±.05	2.871 ±.00	2.021 ±.01	130.6 ±75.	22.30 ±8.3
150	500	2.581 ±.00	2.001 ±.01	3.074 ±.10	2.001 ±.01	2.601 ±.00	2.001 ±.01	50.13 ±4.1	12.31 ±1.8
200	1k	2.187 ±.00	1.942 ±.01	2.304 ±.03	1.941 ±.01	2.192 ±.00	1.941 ±.01	42.77 ±3.8	2.839 ±.62
250	1.5k	2.270 ±.00	1.958 ±.02	2.412 ±.04	1.977 ±.03	2.274 ±.00	1.957 ±.02	42.03 ±3.5	2.511 ±.17
<i>n</i>									
<i>Synth. data with increasing sample size and dimensions fixed at d = 100</i>									
100		2.124 ±.00	1.946 ±.03	78.12 ±24.	2.145 ±.11	2.272 ±.00	1.948 ±.04	58.24 ±4.9	5.346 ±1.9
250		2.802 ±.00	2.018 ±.00	4.489 ±.26	2.025 ±.01	2.871 ±.00	2.019 ±.01	60.27 ±4.1	9.607 ±3.0
500		2.152 ±.00	2.059 ±.04	2.373 ±.08	2.003 ±.05	2.164 ±.00	2.056 ±.04	42.13 ±3.5	3.755 ±.83
1k		2.062 ±.00	1.984 ±.02	2.109 ±.01	2.022 ±.09	2.064 ±.00	1.983 ±.02	39.49 ±3.2	2.608 ±.19
1.5k		2.013 ±.00	2.003 ±.02	2.052 ±.01	2.398 ±1.2	2.014 ±.00	2.001 ±.02	37.19 ±2.9	3.954 ±.77
<i>n</i>									
<i>Twins (d = 48) with increasing sample size</i>									
500		0.182 ±.00	0.151 ±.00	1.161 ±.20	0.168 ±.02	0.183 ±.00	0.151 ±.00	134.6 ±12.	0.842 ±.22
1k		0.196 ±.00	0.159 ±.00	0.261 ±.02	0.172 ±.01	0.196 ±.00	0.159 ±.00	58.70 ±4.4	0.455 ±.14
1.5k		0.166 ±.00	0.156 ±.00	0.171 ±.01	0.159 ±.00	0.166 ±.00	0.156 ±.00	29.72 ±2.4	0.415 ±.14
2k		0.163 ±.00	0.153 ±.00	0.319 ±.04	0.157 ±.00	0.163 ±.00	0.153 ±.00	176.0 ±13.	0.601 ±.30
2.5k		0.169 ±.00	0.162 ±.00	0.321 ±.04	0.164 ±.00	0.169 ±.00	0.162 ±.00	207.8 ±17.	0.479 ±.19
<i>n</i>									
<i>IHDP (d = 25) with increasing sample size</i>									
100		1.807 ±.00	1.673 ±.02	5.933 ±1.2	2.456 ±.47	1.739 ±.00	1.675 ±.02	23.56 ±3.2	14.19 ±9.3
250		1.659 ±.00	1.579 ±.03	2.883 ±.12	2.426 ±.09	1.693 ±.00	1.577 ±.03	11.01 ±2.0	7.985 ±3.1
500		1.625 ±.00	1.614 ±.01	1.819 ±.16	1.673 ±.09	1.641 ±.00	1.610 ±.02	6.614 ±.59	5.602 ±1.6

Table 6: **Copy of Table 1 with additional data (IHDP).** To save space, we include the “complete” table of our main experiment here, in our supplemental material. The content of this table is exactly the same as in Table 1, except for added results on IHDP (bottom block).

Methods		X-Learner		DR-Learner		T-Learner		R-Learner	
EBM		✗	✓	✗	✓	✗	✓	✗	✓
d		<i>Synth. data with increasing sample size and increasing dimensions</i>							
50	100	2.309 ±.00	1.994 ±.02	4.594 ±.56	2.017 ±.04	2.441 ±.00	1.993 ±.01	3.194 ±.26	1.982 ±.04
100	250	2.779 ±.00	2.018 ±.01	4.056 ±.32	2.154 ±.39	2.838 ±.00	2.019 ±.01	3.702 ±.23	2.018 ±.01
150	500	2.618 ±.00	2.000 ±.01	3.030 ±.12	2.001 ±.01	2.641 ±.00	2.000 ±.01	2.877 ±.08	2.000 ±.01
200	1k	2.185 ±.00	1.940 ±.01	2.283 ±.02	1.941 ±.01	2.189 ±.00	1.939 ±.01	2.271 ±.01	1.940 ±.01
250	1.5k	2.267 ±.00	1.949 ±.02	2.427 ±.01	1.976 ±.00	2.271 ±.00	1.948 ±.01	2.436 ±.02	1.949 ±.02
n		<i>Synth. data with increasing sample size and dimensions fixed at $d = 100$</i>							
100		2.134 ±.00	1.927 ±.01	24.61 ±9.9	2.096 ±.09	2.279 ±.00	1.929 ±.01	3.192 ±.13	1.925 ±.01
250		2.779 ±.00	2.018 ±.01	4.056 ±.32	2.154 ±.39	2.838 ±.00	2.019 ±.01	3.702 ±.23	2.018 ±.01
500		2.155 ±.00	2.056 ±.02	2.334 ±.07	2.273 ±.67	2.166 ±.00	2.053 ±.02	2.271 ±.05	2.056 ±.02
1k		2.059 ±.00	1.964 ±.02	2.105 ±.01	2.016 ±.16	2.061 ±.00	1.964 ±.02	2.086 ±.01	1.965 ±.02
1.5k		2.013 ±.00	1.998 ±.02	2.043 ±.01	1.998 ±.02	2.014 ±.00	1.998 ±.02	2.024 ±.01	1.991 ±.02
n		<i>Twins ($d = 48$) with increasing sample size</i>							
500		0.214 ±.00	0.144 ±.00	0.236 ±.04	0.182 ±.05	0.221 ±.00	0.145 ±.00	0.222 ±.02	0.145 ±.00
1k		0.294 ±.00	0.162 ±.00	0.348 ±.12	0.173 ±.03	0.301 ±.00	0.162 ±.01	0.532 ±.11	0.161 ±.00
1.5k		0.165 ±.00	0.154 ±.00	0.189 ±.06	0.159 ±.01	0.165 ±.00	0.154 ±.00	0.172 ±.01	0.154 ±.00
2k		0.167 ±.00	0.156 ±.00	0.197 ±.03	0.159 ±.00	0.167 ±.00	0.156 ±.00	0.222 ±.05	0.157 ±.00
2.5k		0.297 ±.00	0.153 ±.00	0.390 ±.19	0.156 ±.00	0.297 ±.00	0.153 ±.00	0.358 ±.22	0.153 ±.00
n		<i>IHDP ($d = 25$) with increasing sample size</i>							
100		3.369 ±.36	1.783 ±.22	6.484 ±5.7	2.329 ±.67	6.138 ±.50	2.028 ±.65	22.57 ±4.3	16.43 ±9.1
250		47.29 ±.64	2.788 ±1.2	1.899 ±.10	1.689 ±.26	51.76 ±.64	2.963 ±1.3	72.20 ±9.4	54.16 ±22.
500		2.176 ±.25	1.532 ±.01	1.681 ±.04	1.554 ±.02	4.361 ±.35	1.552 ±.03	8.531 ±.94	4.661 ±.75

B.3 Hyperparameters

We report our chosen hyperparameters for each sample-size in Table 7. We found these values through a Bayesian optimization scheme using [Biewald \[2020\]](#). The used ranges are reported in Table 8. As an insight, we noticed that the architecture and amount of noisy samples made little difference to performance in PEHE. The perturbation probability, and the value of k did make a difference, especially in larger sample sizes. Each experiment was performed on an Nvidia GeForce RTX 2080 Ti GPU, and 6 Intel i5-8600K (3.60GHz) CPUs. In some instances we ran independent experiments on a duplicate system.

B.4 Details on benchmarked CATE estimators

We use EconML [Microsoft Research, 2019]⁶ to evaluate the various CATE learners. We keep the hyperparameters for each CATE learner as their default, except for the chosen regression models (which by default are linear). In Table 1 we replace each regressor by a KernelRidge regressor, and each classifier by a support vector machine (SVC); both implemented by [Pedregosa et al. \[2011\]](#). Results on CATE learners with alternative models can be found in Appendix B.2.

⁶EconML is available open-source under an MIT License. Please find all details on their GitHub repository, <https://github.com/microsoft/EconML>.

Table 7: **Chosen hyperparameters for Table 1.** We performed hyperparameter sweeps for each setup using a Bayesian optimisation scheme [Biewald, 2020]. Our searched ranges are reported in Table 8. We have rounded continuous hyperparameters to user-friendly values (as they are sampled from continuous distributions during optimization). Twins settings were also used in Figure 1, but with a fixed $k = 5$ for both AE and EBM. Each integer (separated by a dash) in “Architecture” indicates layer width; “20-20” thus means a neural network with two hidden layers, each of width 20.

Setup	b	k	Architecture	Perturbation prob.
d	n		Synth. data, increasing dim	
50	100	10	3	20-20-20
100	250	10	4	20-20-20
150	500	5	3	20-20
200	1k	3	15	20-20-20-20
250	1.5k	3	20	20-20-20
	n		Synth. data, fixed dim ($d=100$)	
100		5	15	20-20-20-20-20-20
250		10	4	20-20-20
500		3	10	20-20-20-20
1k		3	20	20-20
1.5k		3	10	20-20
	n		Twins, increasing n	
500		5	15	20-20-20-20-20-20
1k		5	16	20-20-20-20-20-20
1.5k		5	16	20-20-20-20-20-20
2k		4	14	20-20-20-20-20-20
2.5k		4	12	20-20-20-20-20-20
	n		IHDP, increasing n	
100		1	5	36-36-36-36-36-36
250		1	5	36-36-36-36-36-36
500		1	5	36-36-36-36-36-36

Table 8: **Ranges for hyperparameter sweeps, for Table 7.** For each setup: (I) Synth. data, increasing dim, (II) Synth. data, fixed dim ($d=100$) (III) Twins, increasing dim, and (IV) IHDP, increasing dim; we used a Bayesian optimization (BO) scheme to find our selected hyperparameters. We chose BO as training representations can get expensive. In or BO setup, we maximized the validation loss which is computed exactly as Equation (3) on a (20%) validation-set.

Setup	b	k	# layers	Perturbation prob.
(I)	$\mathcal{U}(1; 2; \dots; 10)$	$\mathcal{U}(3; 4; \dots; 25)$	$\mathcal{U}(2; 3; 4; 5; 6)$	$\mathcal{U}(0.2; 0.8)$
(II)	$\mathcal{U}(1; 2; \dots; 10)$	$\mathcal{U}(3; 4; \dots; 25)$	$\mathcal{U}(2; 3; 4; 5; 6)$	$\mathcal{U}(0.2; 0.8)$
(III)	$\mathcal{U}(1; 2; \dots; 10)$	$\mathcal{U}(3; 4; \dots; 25)$	$\mathcal{U}(2; 3; 4; 5; 6)$	$\mathcal{U}(0.2; 0.8)$
(IV)	$\mathcal{U}(1; 2; \dots; 10)$	$\mathcal{U}(3; 4; \dots; 25)$	$\mathcal{U}(2; 3; 4; 5; 6)$	$\mathcal{U}(0.2; 0.8)$